Fuel Consumption Prediction Methodology for Early Stages of Naval Ship Design

by

Eran Gheriani

Bachelor of Science in Mechanical Engineering
Tel Aviv University, 1999
Master of Engineering in Systems Engineering
Technion Israel, 2006

Submitted to the Department of Mechanical Engineering in Partial Fulfillment of the Requirements for the Degrees of
Master of Science in Naval Architecture and Marine Engineering
and
Master of Science in Mechanical Engineering
at the
MASSACHUSETTS INSTITUTE OF TECHNOLOGY
February 2012

Signature of author___ _____
Department of Mechanical Engineering
January 9,2012

Certified by__ _____
Chryssostomos Chryssostomidis
Doherty Professor of Ocean Science and Engineering
Professor of Ocean and Mechanical Engineering
Thesis Supervisor

Accepted by_____ _____
David E. Hardt
Professor of Mechanical Engineering
Chairman, Departmental Committee on Graduate Students

Fuel Consumption Prediction Methodology for Early Stages of Naval Ship Design

Abstract

In recent years, fuel consumption has increased in importance as a design parameter in Navy ships. Economical fuel consumption is important not only for operating cost measures but also for ship endurance tankage requirements. Minimizing fuel consumption has many benefits for both naval and commercial ships. This thesis work will suggest a new comprehensive approach to early-stage ship design to determine fuel consumption for the whole system.

A hull must be designed to work harmoniously with an optimized propulsor and propulsion plant to ensure best performance and to comply with imposed design requirements. Thus, this work will address three main aspects of the fuel consumption equation:

- Ship's resistance is calculated using a computational fluid dynamics simulation of the vessel in calm water at various speeds up to maximum speed.
- Propeller performance is based on propeller curves for the chosen propulsor.
- Efficiencies of the drive train and electrical production and distribution system are calculated for all operating conditions. Note that for an electric-drive ship, the non-propulsion electrical loads must be included in the calculations.

These three major components of the ship efficiency equation are assessed for each speed and battle condition of the mission profile. In addition, the corresponding operating conditions for each piece of machinery will be specified to estimate the total fuel consumption and tankage required.

In this thesis work, I will suggest a design methodology to determine hull resistance and total power for a given ship with a specified operational profile. The total power for the operational profile will be translated to fuel consumption, thus producing annual fuel consumption requirements and recommended tankage to support the operational needs.

Thesis advisor: Chryssostomos Chryssostomidis
(Professor of Mechanical and Ocean Engineering)

Acknowledgments

I would like to express my gratitude to my thesis advisor, Professor Chryssostomos Chryssostomidis for giving me the opportunity to take a part in designing the future tools for naval ship design.

To Professor Stefano Brizzolara for the support, for contributing from his knowledge and experience, and for spending so many hours in guiding me towards the desired results and quality.

I would like to express a special thanks to Dr. Julie Chalfant for her contribution of knowledge and experience to this work.

For their mentoring and support during the time of my studies I am grateful to:

Captain Mark S. Welsh, USN
Captain Mark Thomas, USN
Commander Pete R. Small, USN

I would also like to thank the Israeli Navy for giving me the opportunity to experience the academic life at MIT and for sponsoring my graduate studies during this period.

In addition support for the leasing of the software and the purchase of the computer used in this thesis, I wish to thank the Department of Commerce project NA100AR4170086 and the Office of Naval Research projects N00014-11-1-0598 and N00014-08-1-0080.

Last but not least, I would like to express my deepest appreciation and love toward my wife Einat for her infinite support, to our kids: Mika and Elai, and to my family back home, for supporting from far.

This thesis is dedicated to my father, who taught me so much and gave me the tools to be who I am and will be, but did not have the chance to enjoy the fruits he seeded.

Table of Contents

List of Figures

List of Tables

Chapter 1 – Introduction

Fuel consumption became in the last few years a critical design parameter in early phases of ship design. Naval ships, which have a large spectrum of operational requirements, need to be also designed to optimize fuel consumption. This thesis work will suggest a new comprehensive approach to ship design in the aspects of still water resistance, propeller optimization, drive train efficiencies and design (to comply to the operational needs) and fuel consumption for the whole system.

Throughout history, ship resistance predictions during design were the key to a successful design. Many methods were developed for that need; some examples include analytic, numerical, and parametric (based on history and experience). Resistance predictions are the base to machinery and drive train design, speed assessments, tankage, annual fuel usage and life cycle cost (LCC) predictions and many more important parameters leading to critical decision making through the design process.

Even today, early stages of design, and preliminary design of a ship, are based on databases of former designs, and empirical calculation based on very few characteristic parameters of the ship.

As years went by, computational science gained power and became a key player in the fields of computational fluid dynamics (CFD) with use of finite volume methods (FVM), and panel method calculations. Even so, it is still uncommon to find the use of CFD methods for preliminary design.

This thesis work suggests a methodology for early design resistance calculation based on commercial CFD software (STAR CCM+) being used as a replacement for an expensive tow tank test which is usually done in much later stages of design. The results, which are well correlated with tow-tank tests, prove the efficiency (price of calculation vs. accuracy of results) of the method, which is also the foundation for annual fuel consumption prediction (for a specific operational profile), endurance, and tankage calculations.

This thesis lays out the whole methodology starting with the CFD-based resistance calculation, through engine load predictions and fuel consumption assessment for given conditions.

In an era where fuel consumption is a critical parameter in design, and has many environmental aspects, an early accurate prediction is valuable and desired. The thesis is organized as follows: Chapter 1 provides a graphical view of the methodology for a model ship based and Full scale based methodology. Chapter 2 describes the CFD resistance calculation for a model ship Chapter 3 demonstrates the transformation from model scaled ship to full scale, and calculates the bare hull resistance. Chapter 4 shows the calculation made for the propeller power, efficiencies and cavitation. Chapter 5 discusses the drive train, efficiencies, and power distribution methods and calculates the total brake power requests from the engines. Chapter 6 applies the calculation for the ship's fuel consumption and Chapter 7, by using the Navy data sheet, demonstrates the tankage requirements for the ship. Chapter 8 discusses the annual fuel use.

Chapter 9 gathers the conclusions and summation for the report.

Chapter 10 describes further research that is recommended to be complimentary to the work done for this report.

An overview of the methodology is presented on the following pages.

The methodology used for this work (Using model Scale):

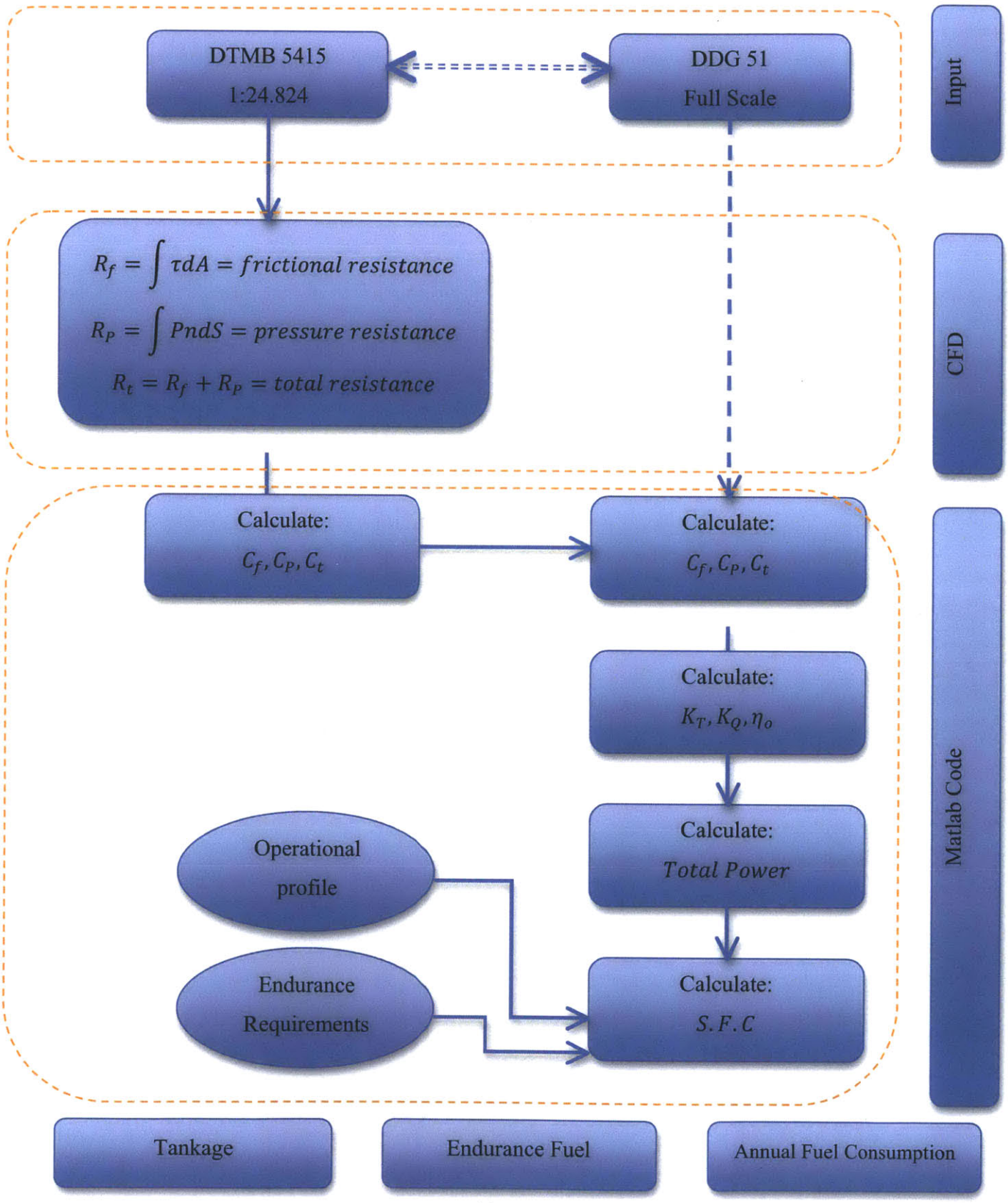

The methodology for a Full scale ship:

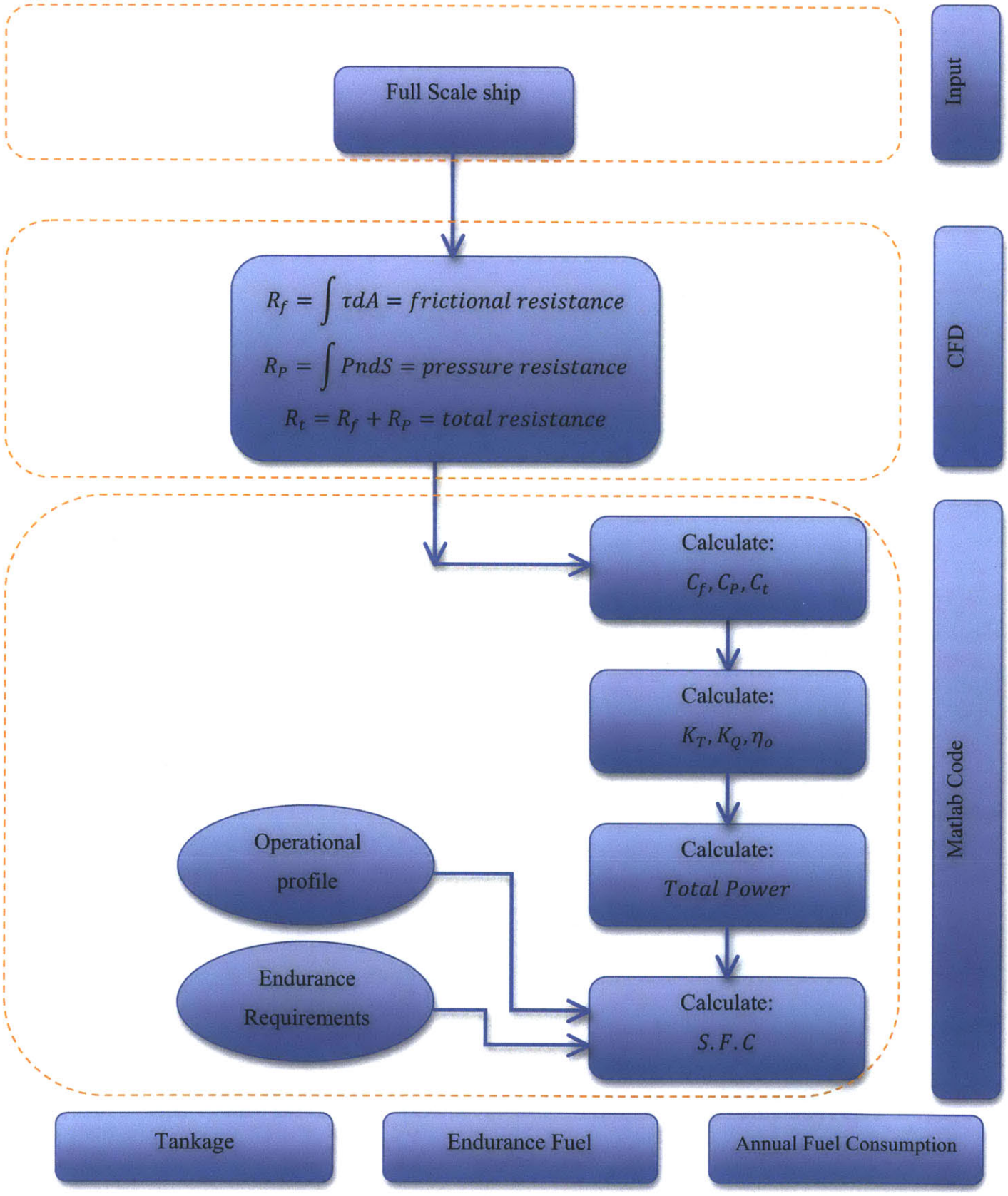

Chapter 2 – Bare-Hull Resistance Calculations

2.1. Background

A ship's hull is a complex structure moving in a stochastic environment like the ocean causing precise resistance calculations to be the "Holy Grail" of ship designers. While traversing the ship design spiral, the naval architect will use various methods to predict the ship's resistance, starting from basic statistical methods based on similarity, data bases, and empirical calculations, through complicated CFD software models, tow tanks for scaled models, and finally a prototype. Despite this process, the ships resistance is known just for the conditions tested, while being exposed in reality to a changing environment and randomly changing conditions. And yet, within that uncertainty, a ship designer should be able to predict the ship's behavior and make sure it complies with specifications.

Ship's resistance force, which is the force needed to tow a ship at a defined speed in water, can be separated into different significant components (Larsson and Raven, 2010):

- Frictional resistance: The ship's hull is moving through a viscous fluid. On the hull, the speed of the water equals the hull's speed (no relative motion). Within a thin layer defined as the boundary layer, viscous forces apply on the hull. The frictional resistance includes the flat plate friction (25%-65% of the total resistance) and a roughness factor (5%-10% of the total resistance).
- Residuary Resistance: All components of resistance not included in frictional resistance, including the form effective pressure resistance (known also as viscous pressure resistance), the form effective friction, and the wave-breaking and wave-pattern resistance.

Alternatively, the total resistance can be divided into viscous resistance (sum of all the members described above but the two wave-related parts) and wave-making resistance, which includes the two members related to waves.

The resistance is often calculated for a bare hull, so resistance components must be added for the appendages and for air resistance of the freeboard and superstructure.

In the early stages of design, after the hull, the propulsors and the drive train are preliminarily designed, it is very common to use a tow tank to validate earlier assumptions and refine the calculation for ship resistance.

Tow tank experiments are an expensive procedure, and some of the tests need to be repeated for statistical analysis (for results deviation and error assessment). Therefore a cheaper, faster and, most importantly, as accurate method to predict full scale resistance forces is highly desired.

CFD (Computational Fluid Dynamics) methods are considered a very powerful, relatively cheap and accurate tool to use for such calculations.

The methodology presented herein will use STAR-CCM+© software to calculate the total resistance of the hull and will be demonstrated on a scaled hull of the DTMB 5415 at scale of 1:24.824. From the scaled hull results the total resistance of a full scale ship will be calculated in a similar process of extrapolating the resistance coefficients from the tow tank results from the scaled model to the real ship.

2.2. The CFD Model

As mentioned, the program that was used for the CFD calculation was STAR-CCM+©, a Generic RANS (Reynolds-Averaged Navier Stokes) Finite Volume solver with the mixture of fluids approach for considering two different fluids – air and water in our case – including pre- and post-processors. Further details can be found in the Gothenberg and Lyngby workshops (Gothenberg workshop, 2010).

The method of modeling we adopt, common in standard CFD programs, is to define the volume of fluid around the body as a control volume using the following process:

a. Import the hull geometry.

b. Build the boundaries of the domain surrounding the hull (can be any desired shape).
c. Subtract the hull geometry from the domain volume.
d. Create the surface and volume meshes.
e. Define the physics and boundary conditions.
f. Define the characteristics.

Each one of the steps needs careful attention to fit the problem.

2.2.1. Hull Geometry

The methodology suggested should be valid for any mono-hull ship. The model tested for the calculation in this work is the DTMB (David Taylor Model Basin) #5415 which is an unclassified hull similar to the DDG-51 combatant. The reason for choosing this specific hull model was the large amount of data available for validation of the predictions, including tow tank test results for different scale models.

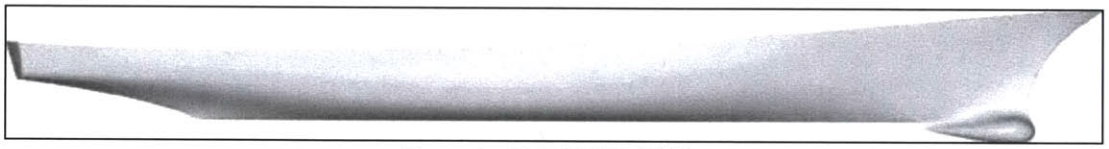

Figure 1 - Hull DTMB 5415

Hull parameters (Basic condition):

Parameter	Symbol	Full scale	Model
Scale factor	λ	-	24.824
Length between perpendiculars	$L_{PP}(m)$	142.0	5.720
Length at water level	$L_{WL}(m)$	142.0	5.720
Overall length	$L_{OS}(m)$		
Breadth	$B(m)$	18.09	0.76
Draft	$T(m)$	6.16	0.248
Trim angle	(deg)	0.0	0.0
Displacement	$\Delta(t)$	8636.0	0.549
Volume	$\nabla(m^3)$	8425.4	0.549

Wetted surface	$S_W(m^2)$	2949.5	4.786

Table 1 - DTMB 5415 parameters

The hull geometry was originally modeled in a CAD program (Rhinoceros©) in full scale and was scaled to the right model size.

Then it was meshed to an STL (Stereo lithographic triangular elements) format file so it can be imported into Star-CCM+.

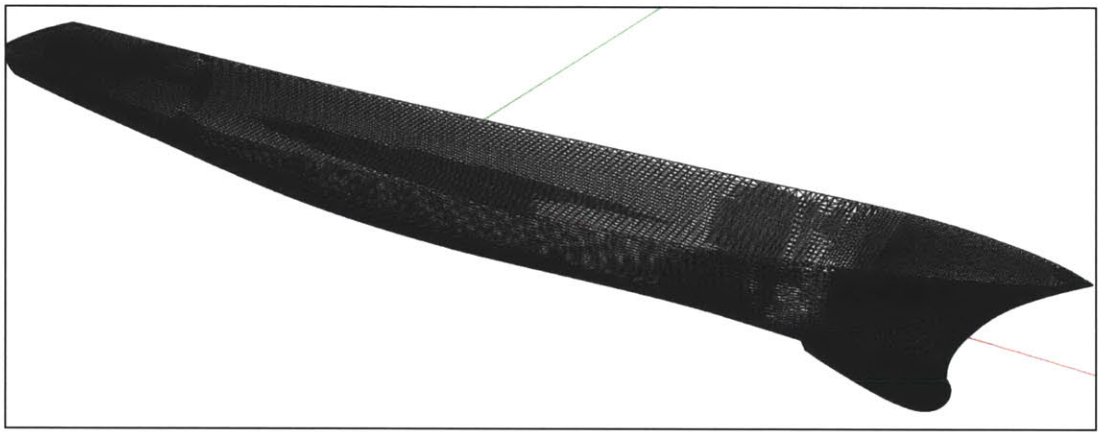

Figure 2 - Hull DTMB 5415 (STL mesh)

While meshing, it is important to pay attention to areas that might experience flow acceleration, high turbulence, or create vortices such as sonar dome/bulbous bow, bilge keels and around any complicated geometry.

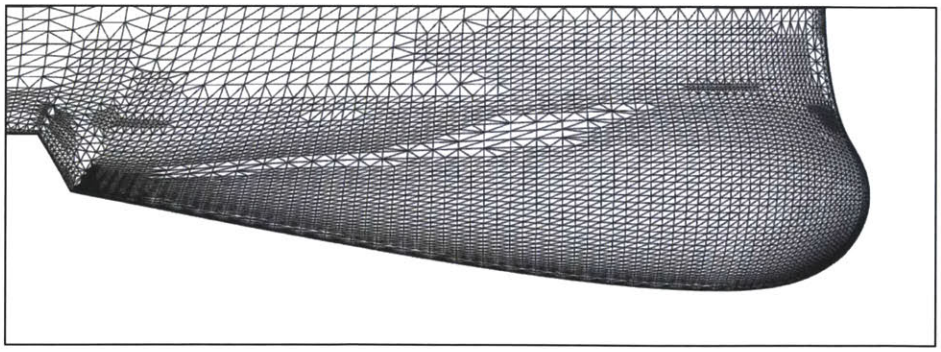

Figure 3 – Sonar dome finer mesh

Another point to notice is that the geometry model, which is made up of surfaces, must be closed without overlapping or incorrectly connected surfaces. Any case where the surfaces are connected poorly will result problems while generating the volume mesh for the CFD calculation.

Star-CCM+ includes a surface/element fixing tool, but it is highly recommended to import the CAD in a final form so element and surface adjustments will not be a necessity.

2.2.2. Control volume – Volume of fluid

One of the most important decisions taken into the design of the domain of fluid and air around the hull is its optimal size. A volume which is too large will add many elements (cells), hence many unnecessary equations to solve, for less interesting parts of the problem. Even selecting a gradual growth of cell size from the hull outwards might not help or may even reduce the accuracy in points of interest.

A volume that is too small will have an effect on the results due to the influence of conditions imposed on the boundaries that normally are true at infinite distance.

Therefore, the size should be just right and planned carefully. Trial and error can verify that the volume is not too small.

For the DTMB 5415, the width of the volume to port and starboard was selected as the same dimension as the tow tank, which is 9 meters ($y = \pm 4.5$).

For the X dimension, one ship's length towards the bow (X+) was modeled, measured from mid-ship, and about two ship's lengths towards the stern, measured also from mid-ship.

On the vertical axis, it is recommended to define the water-plane as the symmetry plane for water and air; that choice makes the calculation of the free surface more accurate since the elements are either air or water and not mixed (water and air elements have a separating surface at the waterplane).

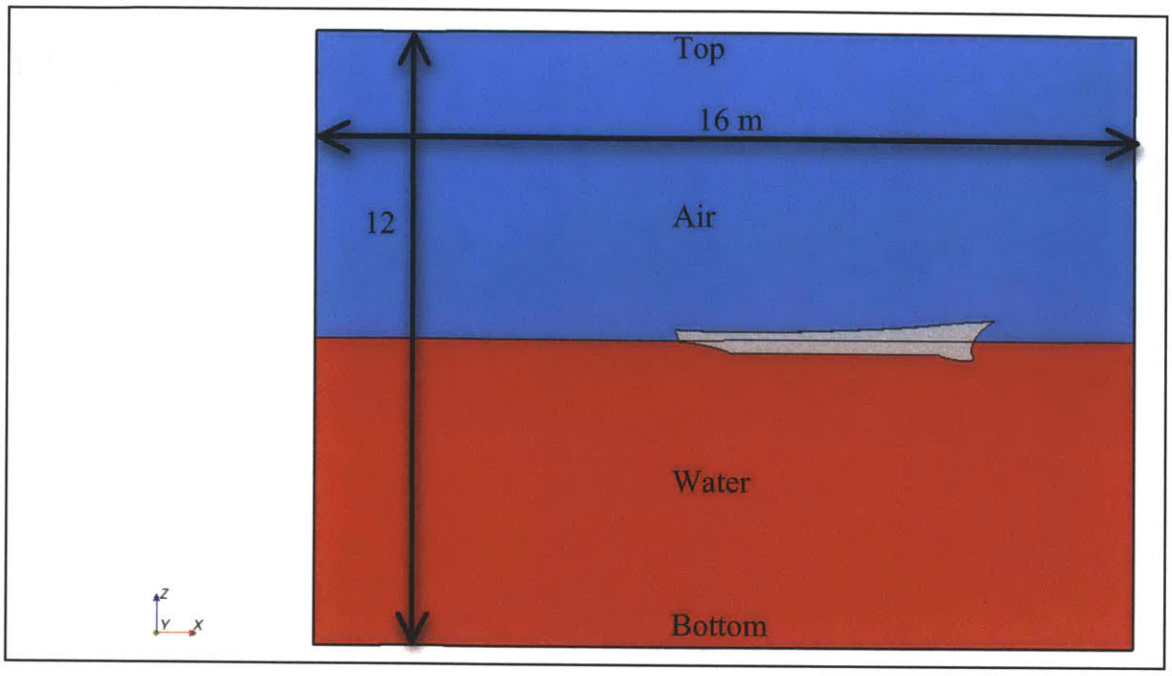

Figure 4 – Control volume around the hull (side view)

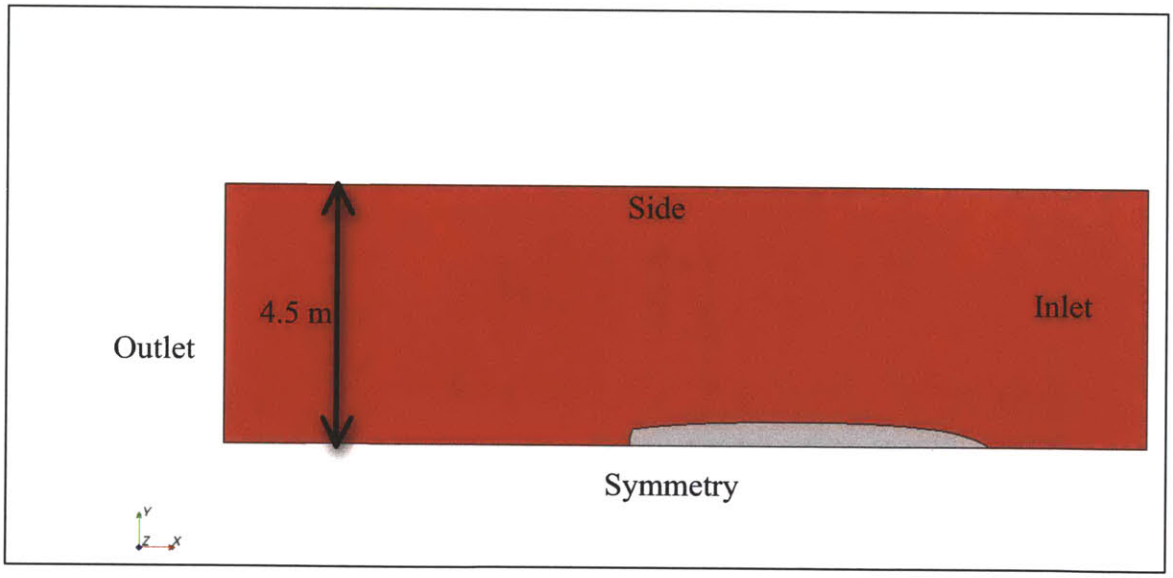

Figure 5 – Control volume around the hull (top view)

2.2.3. Boundary Conditions

The boundary conditions on each surface are set up as follows:

Hull - The boundary condition on the hull is a no-slip condition (zero relative speed) and no flow penetration into the wall (in the normal direction).

Inlet – At the inlet, the flow velocity is uniform and defined. The frontal area of the boundary block was defined as a velocity inlet condition, with the magnitude of the velocity set equal to the ship speed and the direction defined as into the block. The height of water plane and hydrostatic pressure are also defined for the inlet plane.

Outlet – On the outlet area surface, a pressure outlet was defined to allow continuous flow simulation exiting the block, with zero gradient on the flow variables and mean hydrostatic pressure. The initial condition was defined as hydrostatic pressure only.

Symmetry plane – The model was designed for half the ship, which allows better mesh around the hull for given number of cells. A symmetry plane was defined to reflect all data for the other side of the ship.

Top – Defined as pressure outlet to avoid any influence of the boundary on the air flow.

Side wall – Defined as a symmetry wall to create conditions close to unbounded fluid. Despite this, it is clear that numeric inaccuracies will create reflections from the wall making it closer to a real tow tank condition. A wall condition could also be defined but, due to the Venturi effect that can create transverse forces (due to acceleration of fluid between the hull and the wall), it seemed less accurate.

Bottom – We chose a symmetry boundary condition (that is equivalent to a slipping wall condition) to avoid unnecessary calculations of the boundary layer effect in this region.

Allocation of the surfaces is shown in Figures 4 and 5.

2.2.4. Meshing and Evaluating Mesh Quality

The key to create an accurate calculation with FVM (Finite Volume Methods) is the quality and efficiency of the mesh.

A mesh that is too fine (with very small cells) might produce good results but the time it takes to run can be very long and will require small time steps to satisfy the Courant number criteria. On the other hand, a coarse mesh might produce faster calculations but result in incorrect results or even a total crash of the simulation.

For Star-CCM+©, and most other CFD programs, a mesh can be imported from meshing programs like Gambit, GridGen and many others, but Star-CCM+ also includes a meshing module to create the surface and volume meshes. We used the Star-CCM+ meshing module to mesh the DTMB 5415.

For a model of a ship it is highly important to base the size of the cells on physical understanding of the problem and the properties of the mesh. Gradual growth of cell size reduces the total number of elements inside the volume of fluid while allowing smaller elements to be close to area of interest, e.g. for the boundary layer next to the hull.

The process of meshing is based on the hull surface mesh, which should be very fine, and the control volume walls, which can be coarse.

If frictional resistance is an important parameter (and for a ship it is), the boundary layer should be meshed correctly. An important parameter to evaluate the quality of the mesh in the boundary layer around the hull is called **y+** which is a non-dimensional description of distance from a wall in relation to local height of the boundary layer and wall shear stress parameters. The expression of distance from the wall in y+ units is important in defining velocity and turbulence distributions in a universal form suited to wall functions. A very important requirement in the application of wall functions in CFD is that the computational cells adjacent to the wall have a height, usually expressed in y+ units, compatible with the wall functions being employed (A. de Souza, 2005).

An important parameter is the wall shear stress τ_w (drag per unit area). Like any other stress this has dimensions of $[density]\times[velocity]^2$ and hence it is possible to define an important velocity scale called the friction velocity u_τ (can also be written u*):

$$u_\tau = \sqrt{\frac{\tau_w}{\rho}}$$

Using speed and kinematic viscosity, ν, it is possible to form a viscous length scale $l_v = \nu/u_\tau$. Hence, we may define non-dimensional velocity and distance from the wall in so-called wall units:

$$U^+ = \frac{U}{u_\tau}$$

and:

$$y^+ = \frac{y \cdot u_\tau}{\nu},$$

Where y is the normal distance from the wall to the wall-cell centroid and U is the reference velocity.

The value of y^+ should be under 100 for good quality results when high Reynolds number wall function is used as in our case. Star-CCM+© can show rather simply the y^+ values on the hull.

Another important parameter that should be checked for mesh/time step evaluation is the Courant number, which indicates the relation between the speed of fluid particles and the size of the elements.

For a given flow the Courant number can be calculated as follows:

$$C \geq \Delta t \cdot \sum_{i-1}^{n} \frac{u_{x_i}}{\Delta x_i}$$

where:

- u is the velocity in direction x_i.
- Δt is the time step.
- Δx is the length interval
- i is the dimension index (1D, 2D or 3D).

It is recommended to keep the courant number **lower then 1** by adjusting element size or time step size.

When the model is running, the number of inner iterations and the time step will affect the ability to converge. A large number of inner iterations or the selection of a small time step might help the solution to converge but will increase the calculation time significantly. For that reason the time step should be as large as possible (within allowable Courant number), and the number of inner iterations should be kept low, viewed during the run, and adjusted for optimal value (between 2 to 5).

In any case, it is recommended for any FVM method to check the convergence of numerical results with respect to the mesh density (mesh sensitivity analysis). The mesh should produce converged results, such that a finer mesh will make very little change in the accuracy, and a coarser mesh might reduce the accuracy more significantly. The mesh that should be chosen should be the coarsest mesh that achieves convergence.

2.2.5. Modeling the Physics

Modeling the physics of the problem has an extensive impact on the results. Users must have a thorough understanding of the models used, and of their limitations and assumptions. In this section two significant physical models are discussed: the volume of fluid method and the k-Epsilon turbulence method.

2.2.5.1 Volume of Fluid (VOF) Method

In computational fluid dynamics, the volume of fluid method (or in short VOF method) is a numerical technique for tracking and locating the free surface (or fluid-fluid interface).

It belongs to the class of Eulerian methods which are characterized by a mesh that is either stationary or is moving in a certain prescribed manner to accommodate the evolving shape of the interface. As such, VOF is an advection scheme - a numerical recipe that allows the programmer to capture the shape and position of the interface, but it is not a standalone flow solving algorithm. The Navier-Stokes equations describing the motion of the flow have to be solved separately. The same applies for all other advection algorithms.

The method is based on the idea of so-called fraction function C, which is defined as the integral of the fluid's characteristic function in the control volume (namely, the volume of a computational grid cell). Basically, when the cell is empty, with no traced fluid inside, the value of C is zero; when the cell is full, C = 1; and when the interface cuts through the cell, then $0 < C < 1$. C is a discontinuous function since its value jumps from 0 to 1 when the argument moves into the interior of a traced phase.

The fraction function, C, is a scalar function. While the fluid moves with velocity in three dimensions:,

$$V = [u(x, y, z), v(x, y, z), w(x, y, z)],$$

every fluid particle retains its identity, i.e. when a particle is a given phase, it does not change phase. For example, a particle of air that is part of an air bubble in water remains an air particle, regardless of the bubble movement. Thus we must disregard processes such as the dissolving of air in water. For this to be so, then the substantial derivative of fraction function C needs to be equal to zero:

$$\frac{\partial C}{\partial t} + V \cdot \Delta C = 0.$$

2.2.5.2 Turbulence Model: K-Epsilon ($k - \varepsilon$)

Solving the full time-dependent fluctuating state of the turbulence within the fluid can be a very complicated procedure, and for most applications it is unnecessary. Models based

on mean flow without solving the full state first can be applied and provide sufficiently good results.

The K-Epsilon model selected for this calculation is based on the mean Kinetic Energy of the fluid such that:

$$K = (kinetic\ Energy/unit\ mass) = \frac{1}{2}(U^2 + V^2 + W^2)$$

$$k = mean\ turbulant\ kinetic\ energy = \frac{1}{2}\left(\overline{u'^2} + \overline{v'^2} + \overline{w'^2}\right),$$

where U,V and W are the flow velocity components, and $\overline{u'}, \overline{v'}, and\ \overline{w'}$ the average turbulent boundary layer velocity.

The instantaneous Kinetic Energy $k(t)$ is the sum of K and k.

$$k(t) = K + k$$

The dissipation rate of k is epsilon ($\mathcal{E}$). And:

$$\mu_t = turbulent\ viscosity \propto \frac{k^2}{\mathcal{E}}$$

We then solve two partial differential equations for k and $\mathcal{E}$:

$$\frac{\partial(\rho k)}{\partial t} + div(\rho k U) = div\left[\frac{\mu_t}{\sigma_k} grad[k]\right] + 2\mu_t E_{ij} E_{ij} - \rho\mathcal{E}$$

$$\frac{\partial(\rho\mathcal{E})}{\partial t} + div(\rho\mathcal{E}U) = div\left[\frac{\mu_t}{\sigma_\mathcal{E}} grad[\mathcal{E}]\right] + C_1 \frac{\mathcal{E}}{k}\mu_t E_{ij} E_{ij} - C_2 \rho \frac{\mathcal{E}^2}{k}$$

where

$\sigma_k \approx 1.0(Prandtl\ number)$

$\sigma_\mathcal{E} \approx 1.3\ (Prandtl\ number)$

$C_1 \approx 1.44$

$C_2 \approx 1.92$

The values are the default values for this turbulence model, as given in the Star-CCM+© User Manual (eqn 412).

The CFD program solves the equations at each iteration and calculates the mean viscosity and thus equivalent stresses in the turbulent flow.

2.3. Preparing the CFD Results

When creating the CFD cases, the form of the plots and outputs should be clearly decided in advance. Properly choosing the output parameters will make sure that they are calculated during the process and saved in the results database.

For the cases created for this thesis, the following parameters were pre-defined for review:

- frictional resistance force in the x direction (selected only on hull cells).
- pressure forces in the x direction (selected only on hull cells).
- total force in the x direction (summing the frictional and pressure).
- pitching moment (y direction).
- lift force on the hull (z direction).

The graphical views selected for visualization were:

- Convective Courant number (the speed vs. cell size parameter).
- y+ non-dimensional turbulence (boundary layer mesh evaluation).
- Elevation of the free surface.

Some of the parameters were chosen with the intention to use them for the resistance calculations and others were chosen for evaluation and control of the results during the run of the CFD model.

For easier terminology and commonality to the final methodology, the speeds referenced will be the correlated ship speeds and not the model speed (unless specified otherwise).

2.4. CFD Results

For each (ship) speed from 10 knots to 30 knots (with a 5 knot step), a CFD model was built. The running trim and sinkage were taken from the tow tank test results (reference) average values and applied to the CFD model. The output requested from the CFD run was:

- frictional resistance force (continuously measured)
- pressure resistance force (continuously measured).
- total resistance force (continuously calculated).
- water surface elevation contour plot.

Calculating for speeds lower than 10 knots could not be compared to the tow tank results. The tow tank results for speeds lower than 10 knots seemed not accurate enough for a fair comparison. The result from the towing tank experiments shows a higher resistance force at 5 knots then in 10 knots which does not make real sense.

2.4.1. Speed of 30 Knots (Fr=0.41)

For the speed of 30 knots (Fr=0.41), Figure 6 shows a typical free wave pattern generated by the hull.

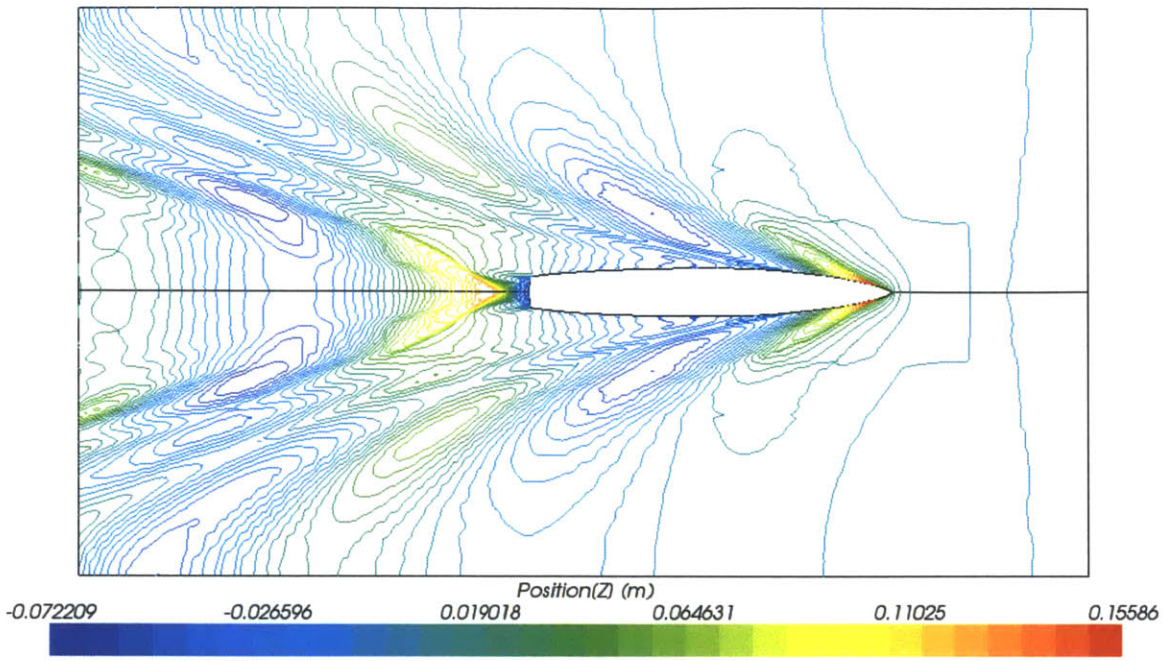

Figure 6 – 30 knots water surface elevation

The peak height of the bow wave as seen in figure 7, created at a constant speed of 30 knots was 0.155 meters. The value is normalized by the length of the ship with a resulting non-dimensional value of 0.027.

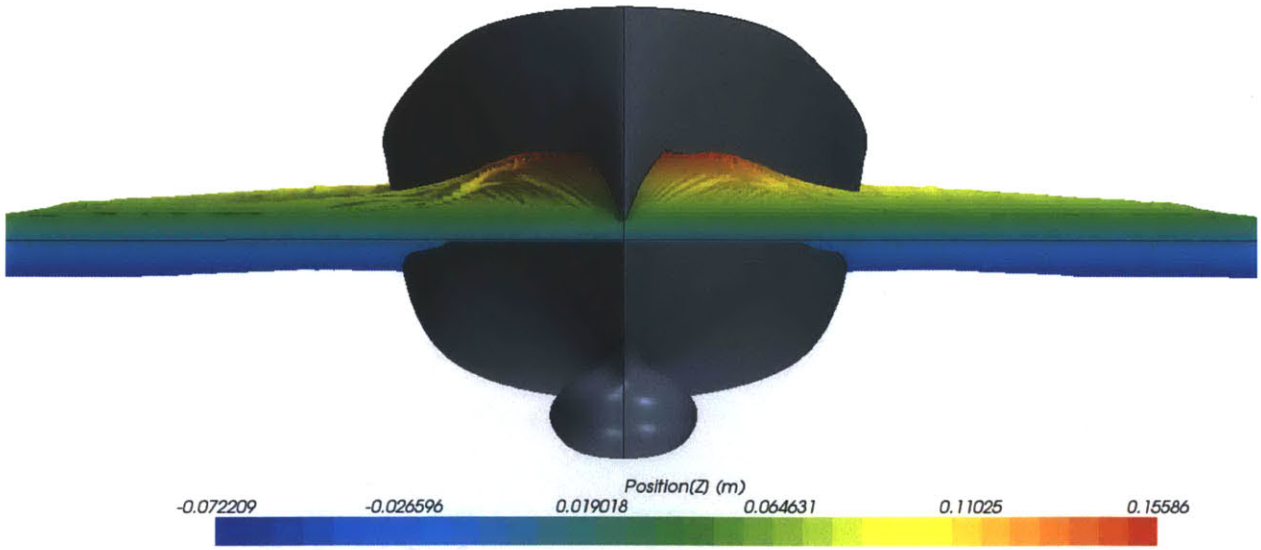

Figure 7 – 30 knots, Bow wave

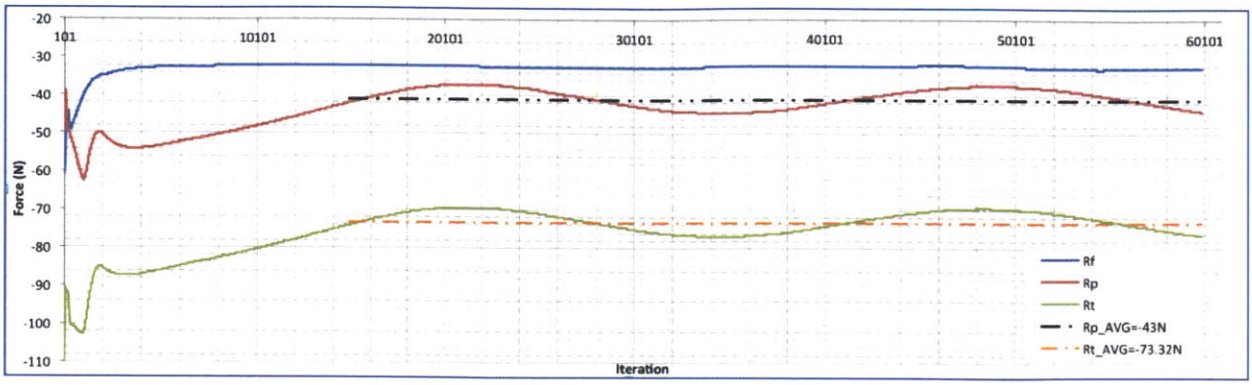

Figure 8 – 30 knots, Resistance force components plot

Figure 8 shows an oscillation in the results for the pressure force, which makes the total force oscillate as well. The phenomenon of the oscillation will be discussed and elaborated in the next chapters of this report.

Input and results are summarized in Table 2. Note that the raw CFD results as presents in figure 8 were for half the hull (symmetry assumption for calculation efficiency). The results in table 2 are already multiplied by factor of two.

Model speed(m/s)	Ship Speed (kts)	Froude Number	Trim (deg) (constant)	Sinkage (m) (constant)	Friction Force $R_f(N)$	Pressure Force $R_P(N)$	Total Resistance $R_T(N)$
3.071	30	0.41	-0.42	0.026	64	82	164

Table 2 – 30 kts CFD result summary

2.4.2. Speed of 25 Knots (Fr=0.34)

This section provides the results for the speed of 25 knots (Fr=0.34).

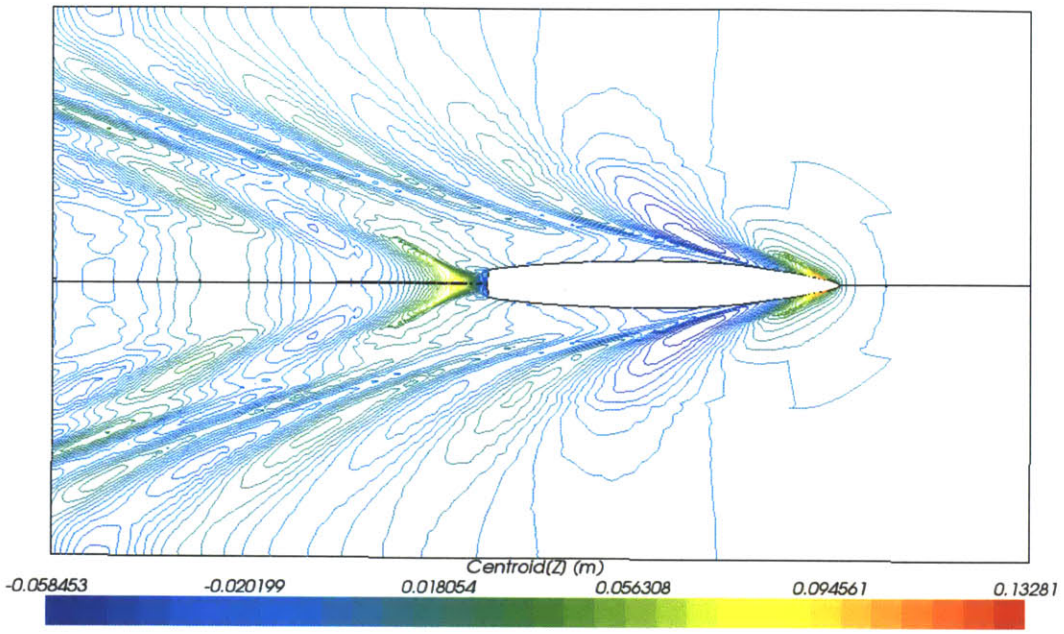

Figure 9 – 25 knots water surface elevation

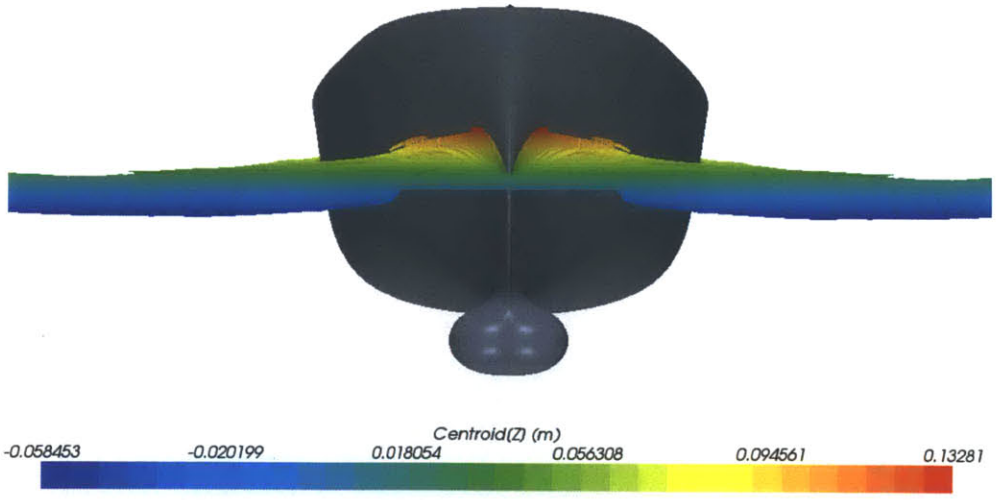

Figure 10 – 25 knots Bow wave

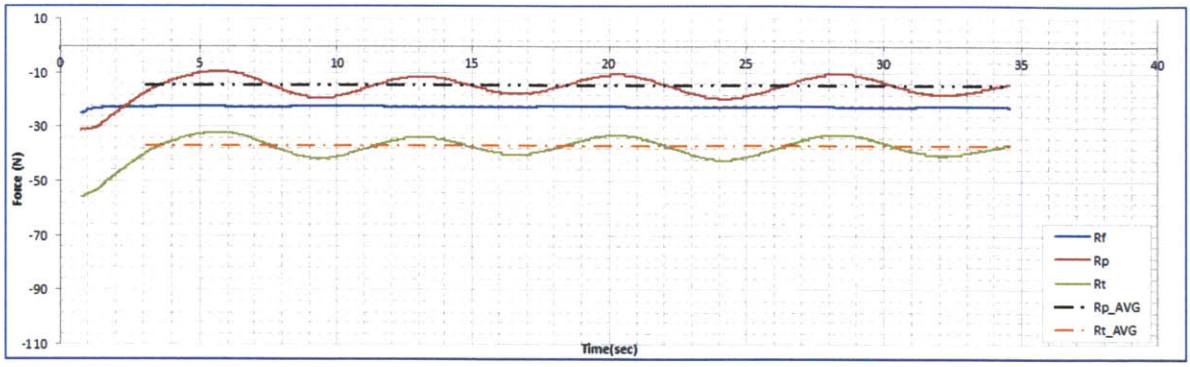

Figure 11 – 25 knots Resistance force components plot

Model speed(m/s)	Ship Speed (kts)	Froude Number	Trim (deg) (constant)	Sinkage (m) (constant)	Friction Force $R_f(N)$	Pressure Force $R_P(N)$	Total Resistance $R_T(N)$
2.54	25	0.34	0.08	0.016	45	32	77

Table 3 – 25 kts CFD result summary

2.4.3. Speed of 20 Knots (Fr=0.28)

This section provides the results for the speed of 20 knots (Fr=0.28).

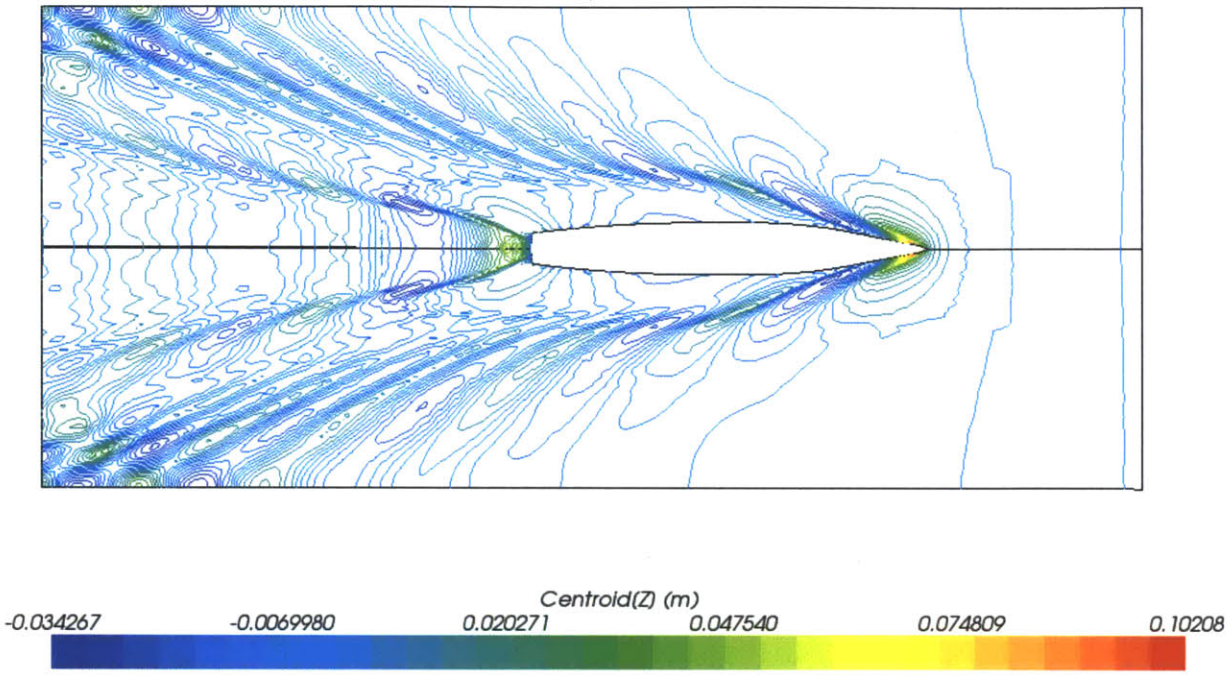

Figure 12 – 20 knots water surface elevation

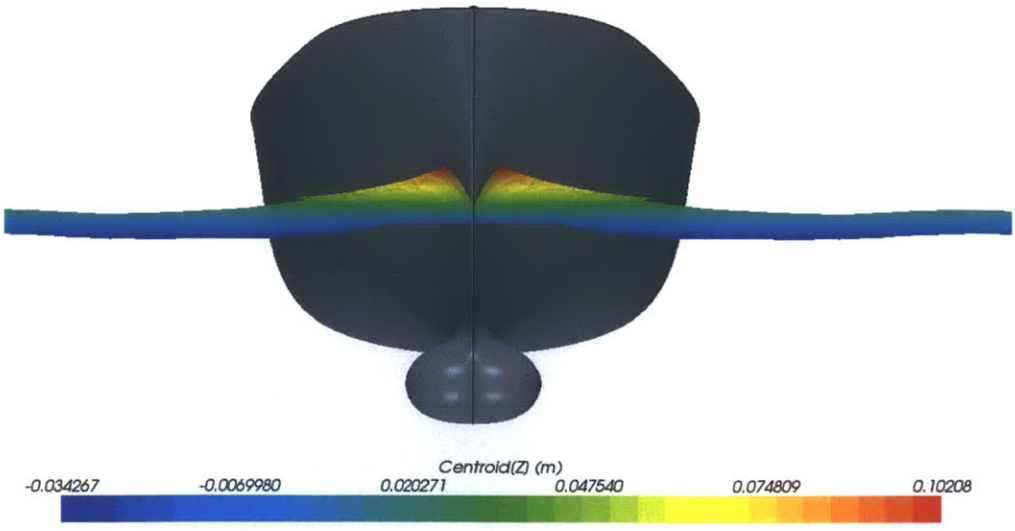

Figure 13 – 20 knots Bow wave

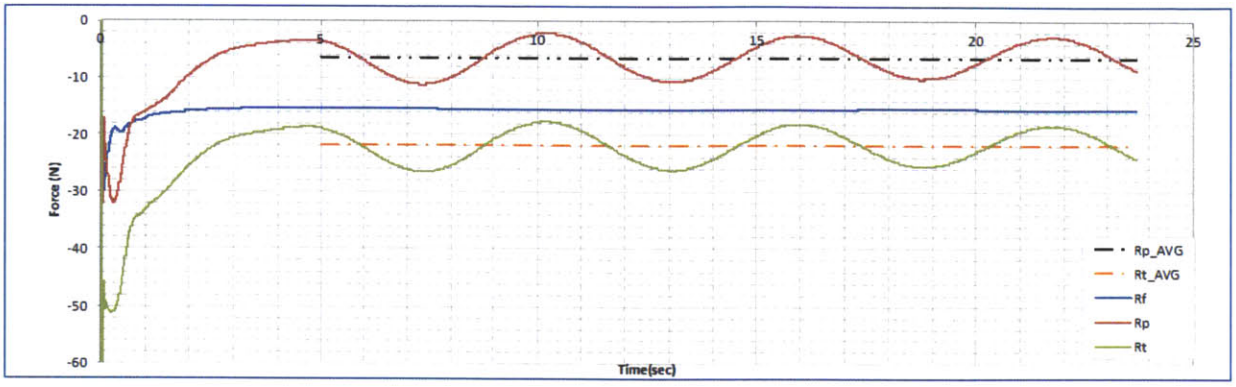

Figure 14 – 20 knots Resistance force components plot

Model speed(m/s)	Ship Speed (kts)	Froude Number	Trim (deg) (constant)	Sinkage (m) (constant)	Friction Force $R_f(N)$	Pressure Force $R_P(N)$	Total Resistance $R_T(N)$
2.097	20	0.28	0.108	0.001	31.12	13.04	44.16

Table 4 – 20 kts CFD result summary

2.4.4. Speed of 15 Knots (Fr=0.20)

This section provides the results for the speed of 15 knots (Fr=0.20).

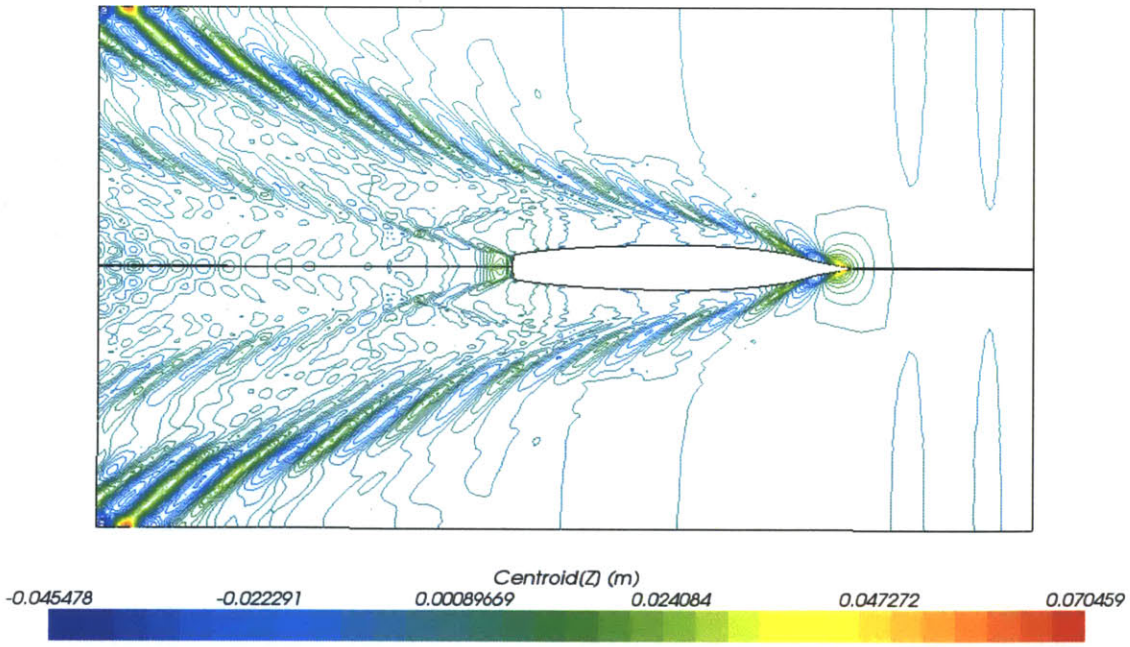

Figure 15 – 15 knots water surface elevation

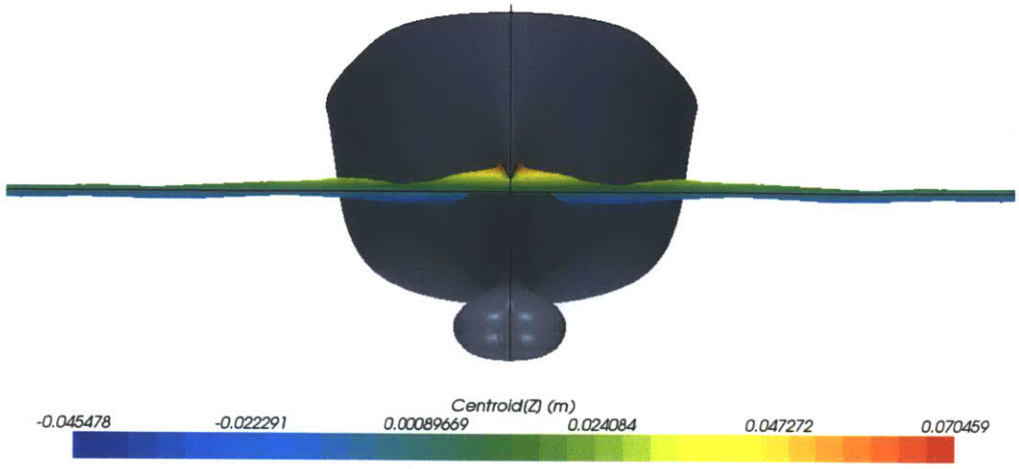

Figure 16 – 15 knots Bow wave

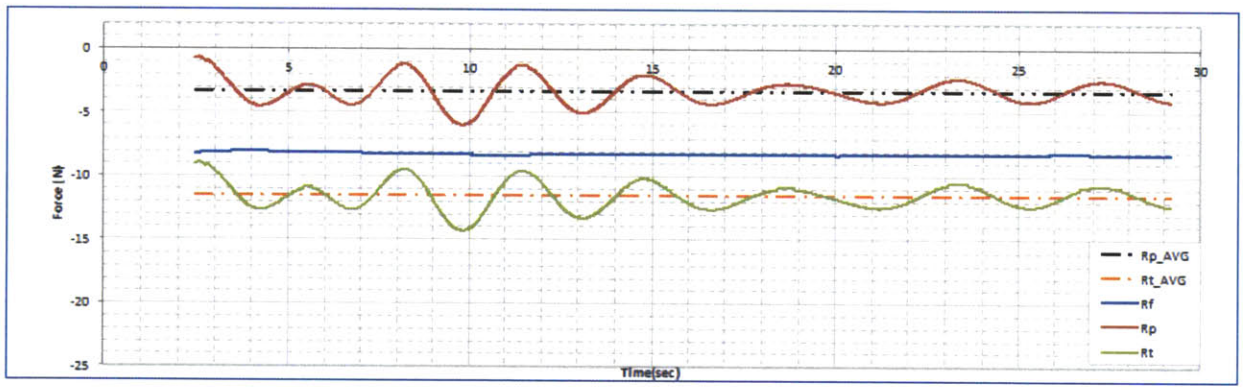

Figure 17 – 15 knots Resistance force components plot

Model speed(m/s)	Ship Speed (kts)	Froude Number	Trim (deg) (constant)	Sinkage (m) (constant)	Friction Force $R_f(N)$	Pressure Force $R_P(N)$	Total Resistance $R_T(N)$
1.501	15	0.2	0.061	0.053	16.22	6.4	22.62

Table 5 – 15 kts CFD result summary

2.4.5. Speed of 10 Knots (Fr=0.14)

For the speed of 10 knots (Fr=0.14), Figure 18 clearly shows the wake form and waves from bow and stern, but also another wave (low amplitude) running from the inlet

backwards. The wave was assumed to be generated from a numeric error in the inlet. It didn't seem to decay in time, so further investigation is needed. Despite this spurious wave, the simulation indicated the average value clearly.

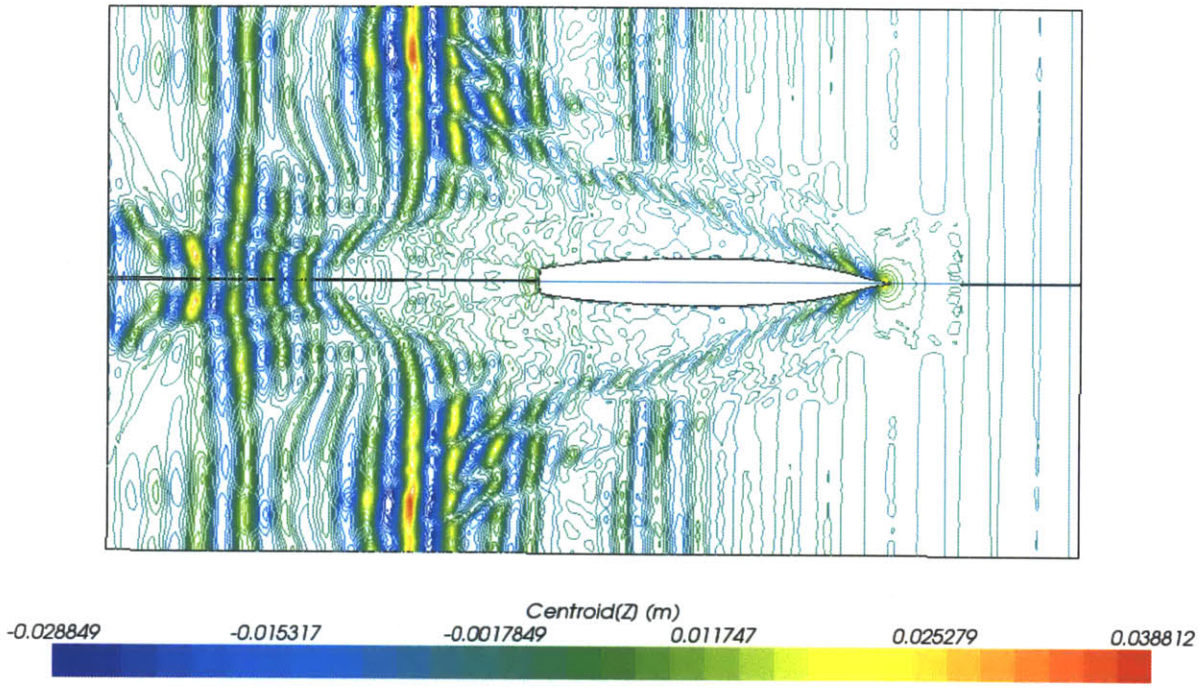

Figure 18 – 10 knots water surface elevation

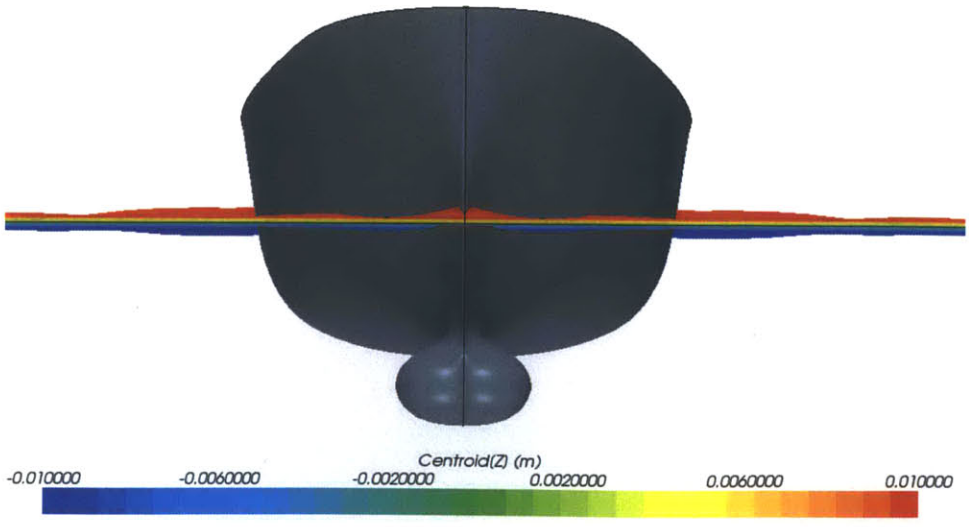

Figure 19 – 10 knots Bow wave

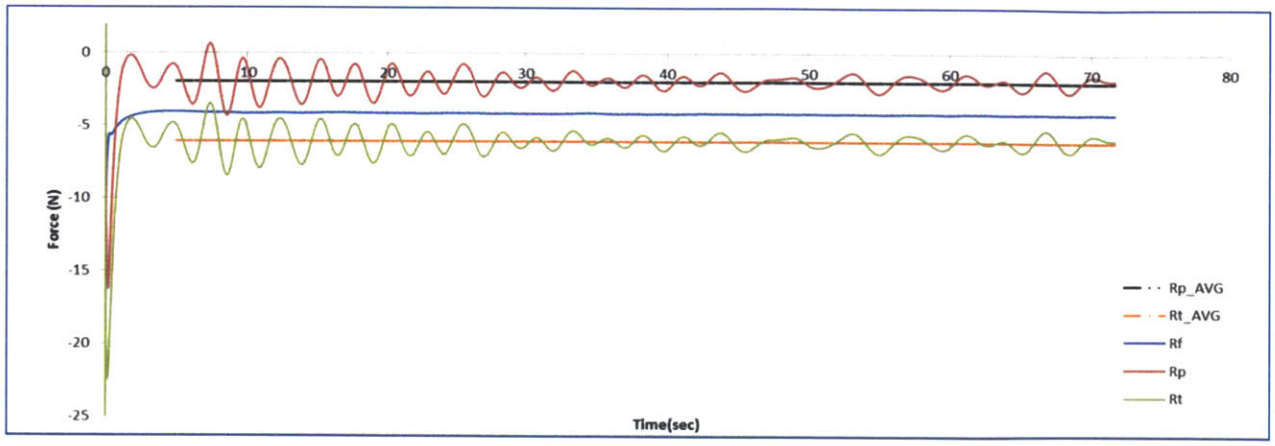

Figure 20 – 10 knots Resistance force components plot

Model speed(m/s)	Ship Speed (kts)	Froude Number	Trim (deg) (constant)	Sinkage (m) (constant)	Friction Force $R_f(N)$	Pressure Force $R_P(N)$	Total Resistance $R_T(N)$
1.03	10	0.14	0.028	0.0025	8.26	3.88	12.14

Table 6 – 10 kts CFD result summary

2.5. Comparing CFD to Tow Tank results

2.5.1. Total resistance comparison

Keeping in mind that one of the goals of the methodology presented in that thesis is to replace early stage tow tank experiments with a CFD model, it is necessary to show that the CFD results are accurate enough when compared to the results found in the tow tank.

As mentioned in earlier chapters, the hull that was tested to demonstrate the method was the DTMB 5415 (U.S. Combatant).

Table 7 summarizes the results. The total absolute error for higher speeds (above 20 kts, Fr=0.28) is relatively low – less than 5%. For lower speeds (10 kts and less) we know that the tow tank results may present large errors themselves so no comparison runs were made using CFD.

	Fr	Tow tank			CFD			Error		
Ship Speed (kts)		**Rf(N)**	**Rr(N)**	**Rt(N)**	**Rf(N)**	**Rr(N)**	**Rt(N)**	**Rf%**	**Rr%**	**Rt%**
10.0	0.13	8.470	1.424	9.894	8.200	4.000	12.200	3.182	-180.839	**-23.309**
15.0.	0.20	16.561	4.646	21.207	16.220	6.400	22.620	2.061	-37.760	**-6.663**
20.0	0.28	29.605	13.429	43.034	31.120	13.040	44.160	-5.117	2.898	**-2.616**
25.0	0.34	43.652	29.875	73.527	44.800	30.000	74.800	-2.630	-0.418	**-1.731**
30.0	0.41	62.491	90.189	152.680	64.000	82.000	146.000	-2.414	9.080	**4.375**

Table 7 – Comparing CFD results to Tow Tank Results

The tow tank results for the frictional resistance are the ITTC '57 line. Calculation of the ITTC line is described in Section 2.5. It seems that the ITTC '57 friction line calculation closely approximates the frictional resistance found using the CFD process; differences are very small for this type of hull.

The higher error results occurred in the pressure resistance part of the total resistance.

It can clearly be shown on a comparative resistance curve (Figures 21, 22 and 23) that the total resistance predictions using CFD nicely approximate the tow tank experiments.

The tow tank results present the total resistance force. For comparison sake, the total resistance can be separated into frictional resistance (calculated by the ITTC '57) and pressure resistance (calculated by subtracting the friction resistance from the total). If from some reason the ITTC '57 formula under-predicts the friction resistance, then the residual resistance part will be larger, and the opposite for over-prediction. That is the reason that the real comparison between the experiment and the CFD calculation will be for the total resistance only. For our case it shows that when the frictional resistance calculated by CFD is larger (negative error sign) then the pressure resistance prediction error will have the opposite sign (positive error sign).

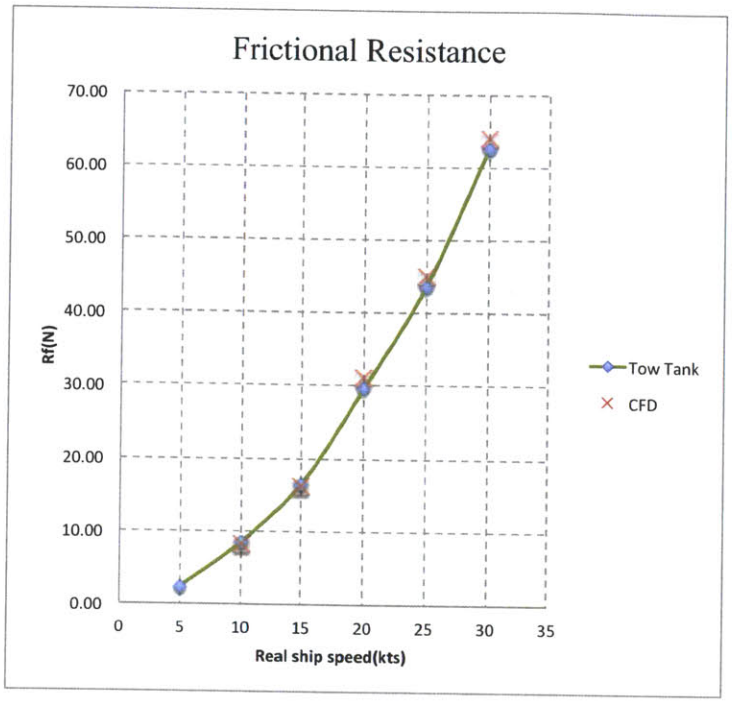

Figure 21 –Friction Resistance (CFD vs. Tow Tank)

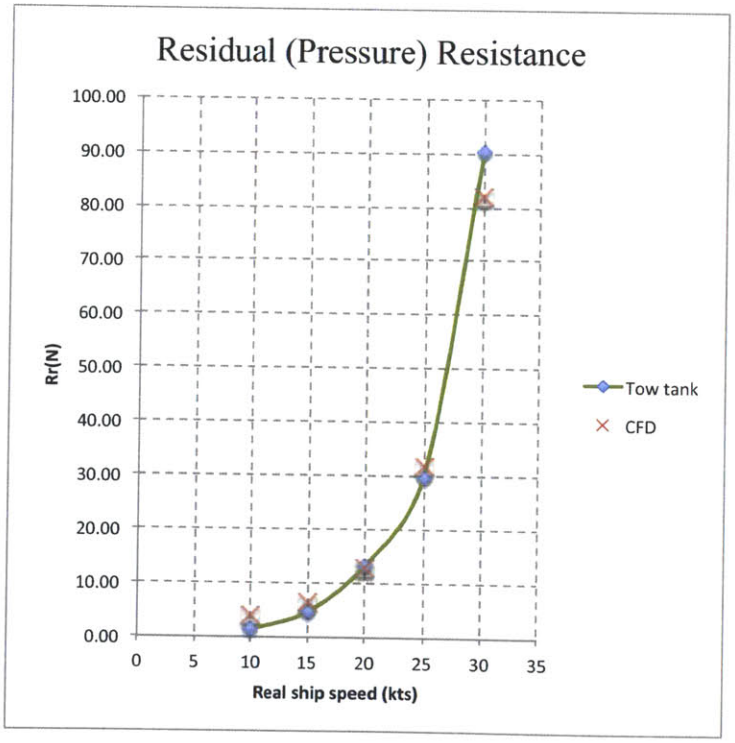

Figure 22 – Pressure Resistance curve (CFD vs. Tow tank)

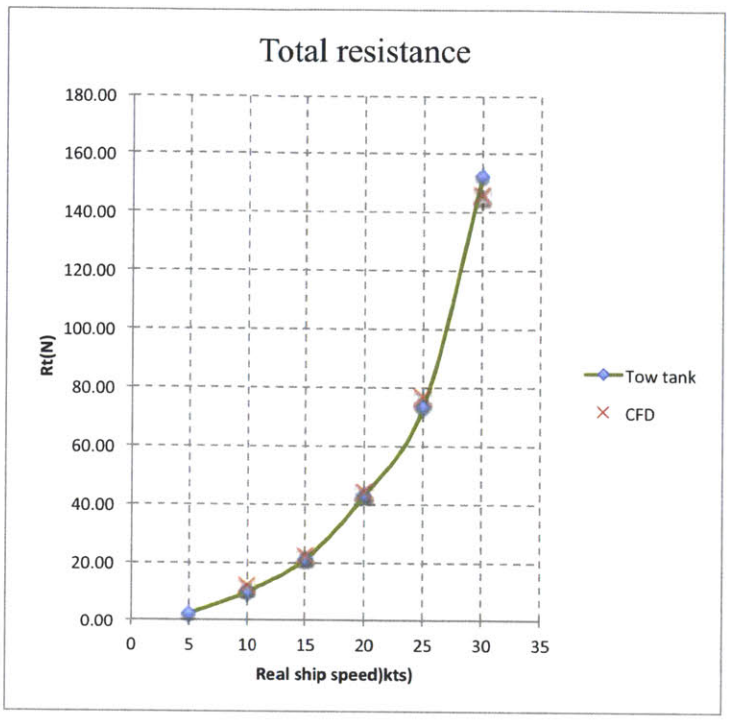

Figure 23 – Total Resistance Curve (CFD vs. Tow Tank)

2.5.2. Wave pattern comparison

The results from the tow tank experiments presented two different analyses for the waves generated by the hull: Wave elevation profile along the hull, and longitudinal wave cuts at three given lateral distances from the hull centerline.

Wave elevation profile – Along the hull.

The wave elevation contour along the hull was measured in the tow tank experiment for two speeds, 20 knots (Fr=0.28) and 30 knots (Fr=0.41). The results were presented in a non-dimensional form, normalized by the length of the ship.

The results in figures 24 and 25 show the tow tank results vs. the CFD results for the speeds discussed above:

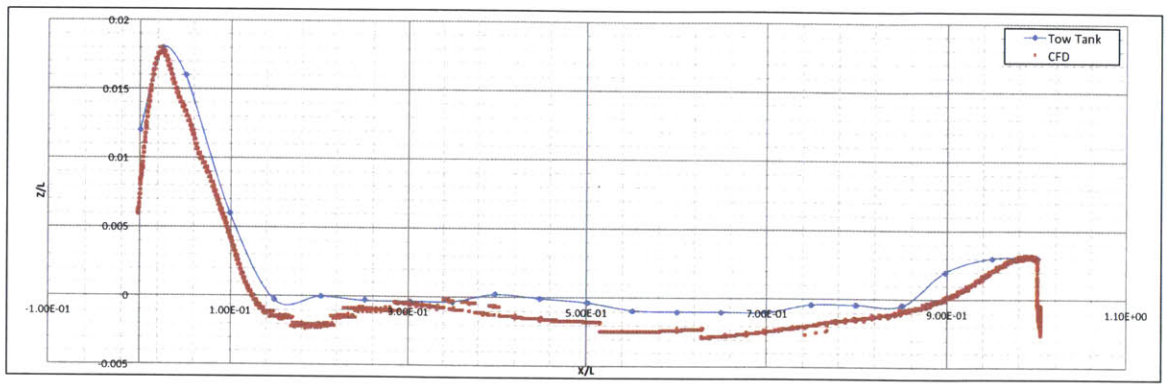

Figure 24 – Wave elevation profile (Fr=0.28)

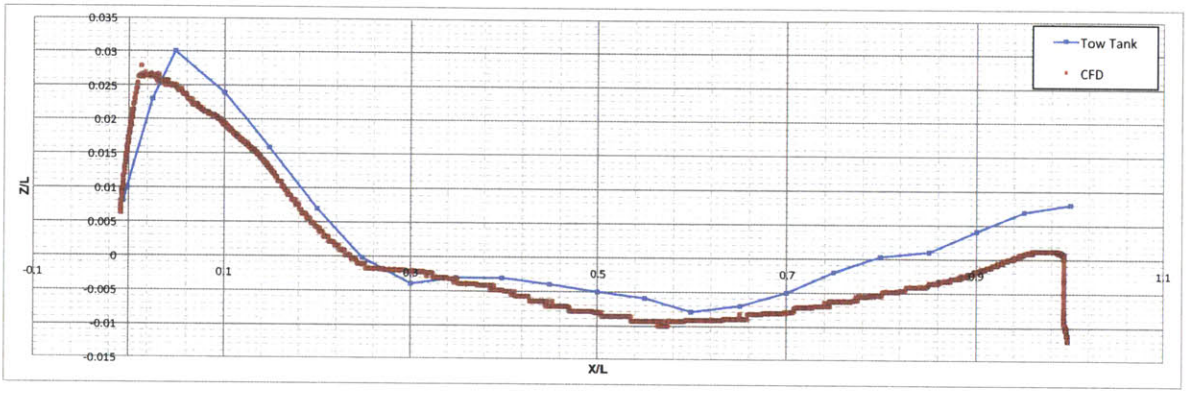

Figure 25 – Wave elevation profile (Fr=0.41)

Figure 24 shows a good correlation of the CFD results with the tow tank measurements, in terms of the first bow wave (peak height) and the wave profile over the entire ship length.

Figure 25 shows some differences, especially at the bow and stern. It seems that the stern wave is not well captured. The difference in the peak height of the bow wave can be partially ascribed to the difficulty to capture and measure the wave which is breaking, as can be seen in Figure 7. The difference at the stern could be also due to underestimating the bow wave which interferes differently with the stern waves.

Longitudinal Wave Cuts

The wave cuts were measured for one speed only – 20 knots (Fr=0.28) – at three different lateral distances from the hull centerline (Y/L=0.082, 0.172, 0.301), as shown in figure

26. Figures 27 and 28 show comparisons of the CFD and tow tank wave cuts at Y/L = 0.082 and 0.172 respectively.

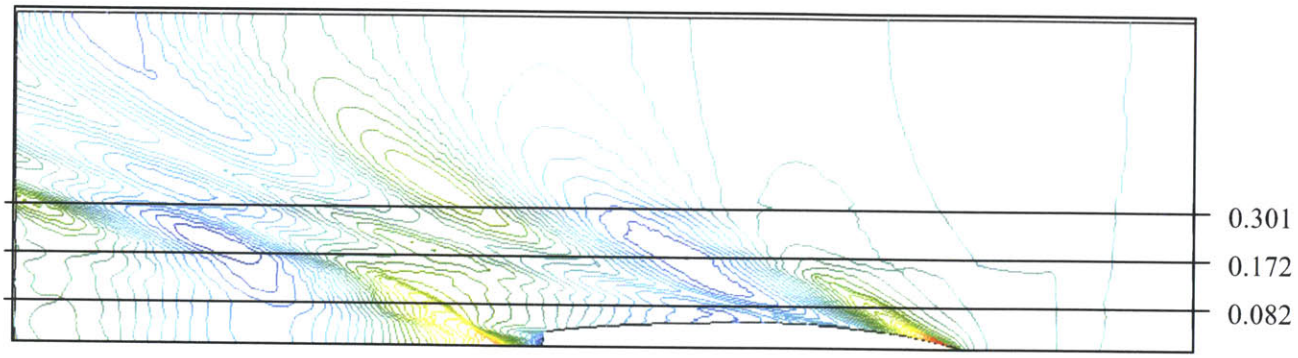

Figure 26 – Wave cut locations

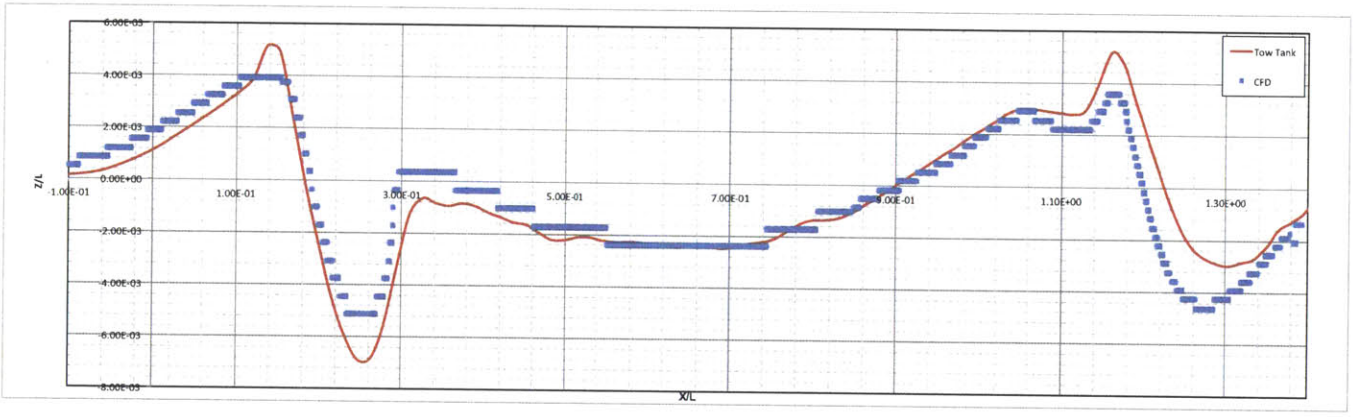

Figure 27 – Wave cut Y/L=0.082

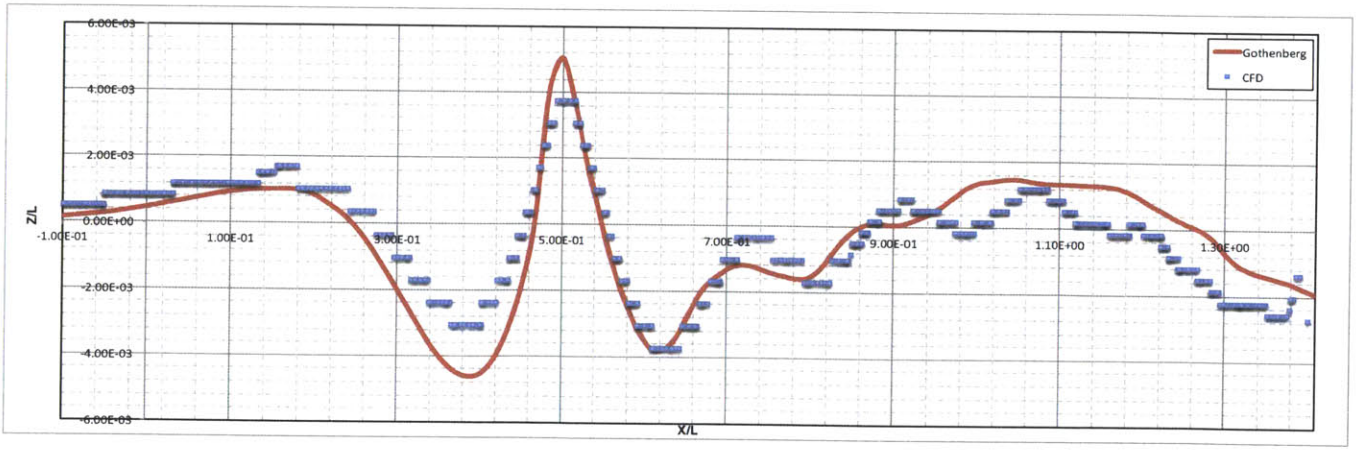

Figure 28 – Wave cut Y/L=0.172

The wave cut for Y/L=0.301 was not used for comparison due to the coarseness of the CFD mesh that was used in the far field of the domain for optimizing the number of elements. It can be seen in Figures 27 and 28 that wave cuts from the CFD results are not smooth curves, but show discrete steps. Each step corresponds to a constant value that is equal to the height of the volume cells used in that area; larger steps indicate larger elements. In the CFD model, it was decided to create a fine mesh near the hull, and a coarse mesh farther away, so wave cuts farther from the hull will have even larger steps.

In the tow-tank report (Olivieri, 2001), the author added a photo of the bow wave at Fr=0.28. The visual comparison in Figure 29 between the CFD and tow-tank results shows a similar bow wave length along the bow and a similar crest length. Note that the sonar dome appears different in the two images due to the refraction of the light as it passes through the water surface in the experiment.

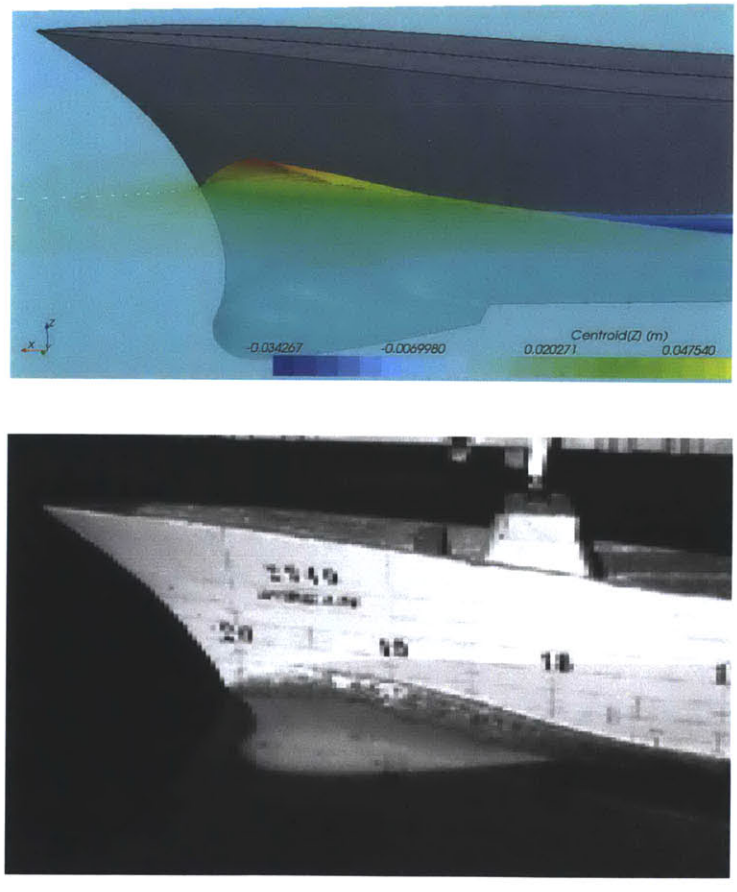

Figure 29 – Bow wave, Fr=0.28 (CFD vs. Tow tank)

2.6 From Model to Ship (Bare Hull)

Since the CFD example run in this work was a scale-model vessel, in order to validate the numerical results, before continuing calculations, the resistance must be projected from the small scale-model to a full size ship as done in tow tank tests. Please note that this section applies to this example only; in full use of this methodology, the CFD model would be full-size and no scaling would be required. The development in this section is a standard method found in many Naval Architecture texts; we refer to (Zubaly 1996).

Based on similarity coefficients, the non-dimensional Froude and Reynolds numbers are:

$$F_n = \frac{V}{\sqrt{gL}} \text{ and}$$

$$R_n = \frac{VL}{\nu},$$

where V is ship or model speed, g is the gravitational constant, L is ship or model length between perpendiculars, and ν is viscosity of the fluid. It is impossible to achieve complete dynamic similitude of the Reynolds and Froude numbers simultaneously between the scale model and the full scale ship due to the inability to change viscosity and gravity in a way that will compensate for the scale difference. Therefore, we separate the Reynolds-dependent part (frictional resistance) and the Froude-dependent part (residual resistance):

$$C_{total} = C(R_n) + C(F_n) = C_{Friction} + C_{Residual} = C_F + C_R = C_T$$

For the scale model:

$$C_{TM} = C_{FM} + C_{RM}$$

And for the full size ship:

$$C_{TS} = C_{FS} + C_{RS}$$

The model is scaled to match Froude numbers, so the Reynolds-dependent resistance is calculated instead of scaled. Since we have similitude in the Froude number and not in Reynolds number, we can say:

$$C_{FM} \neq C_{FS}$$

$$C_{RM} = C_{RS}$$

We get C_{TM} from the CFD/Tow tank model and calculate C_{FM} using the ITTC 1957 line (ITTC 7.5-02-03-01.1, 2002):

$$C_F = \frac{0.075}{(logR_n - 2)^2}.$$

Thus, residual resistance is calculated to be:

$$C_{RM} = C_{TM} - C_{FM}.$$

Although both the frictional and the pressure-caused forces can be obtained directly from the CFD model, we chose to use the ITTC 1957 line to calculate frictional resistance in this case for sake of consistency.

Calculating the ship's frictional force coefficient using the ITTC1957 line and assuming that the residual coefficient of the resistance force is equal for the ship and the model, we can find the total resistance coefficient for the ship:

$$C_{TS} = \left(\frac{0.075}{(logR_n - 2)^2}\right)_S + C_M + C_A,$$

where C_A is the correlation allowance used for a non-perfectly-smooth hull, and is usually taken as 0.0005 (NAVSEA, 1984). The US Navy Design Data Sheet on calm-water resistance, DDS-051 (NAVSEA, 1984), recommends adding 0.0007 as the correlation allowance for two years without dry docking and cleaning (yielding a total correlation allowance of 0.0012). In this work a value of 0.0005 was used for a new hull.

Chapter 3 – Full-Scale Total Resistance

3.1 Background

For a given hull, the bare-hull resistance for ship's speed from zero to maximum desired speed is calculated using STAR-CCM+ CFD software by following the procedure described in Chapter 2 with a full-scale model of the vessel. To obtain total resistance, we must add appendage and air resistance, which are calculated as described in this chapter.

3.2 Appendage Drag

The bare-hull resistance indeed has the largest contribution to the total resistance, but other external appendages can add 10%-30% to the total resistance.

The formula suggested in DDS-051, the U.S. Navy Design Data Sheet for calculating calm-water resistance (NAVSEA, 1984), is based on empirical data collected from other ships and calculates the added power required to overcome the resistance of the appendages:

$$P_{E(AP)} = \frac{L \cdot D_P \cdot V_S^3 \cdot C_{D(AP)}}{K_1}$$

where

L- is the ship length between perpendiculars.

D_P - is the propeller diameter

V_S - is the ship speed

$C_{D(AP)}$ - Is the drag coefficient found from Figure 30

K_1 – is the unit conversion constant.

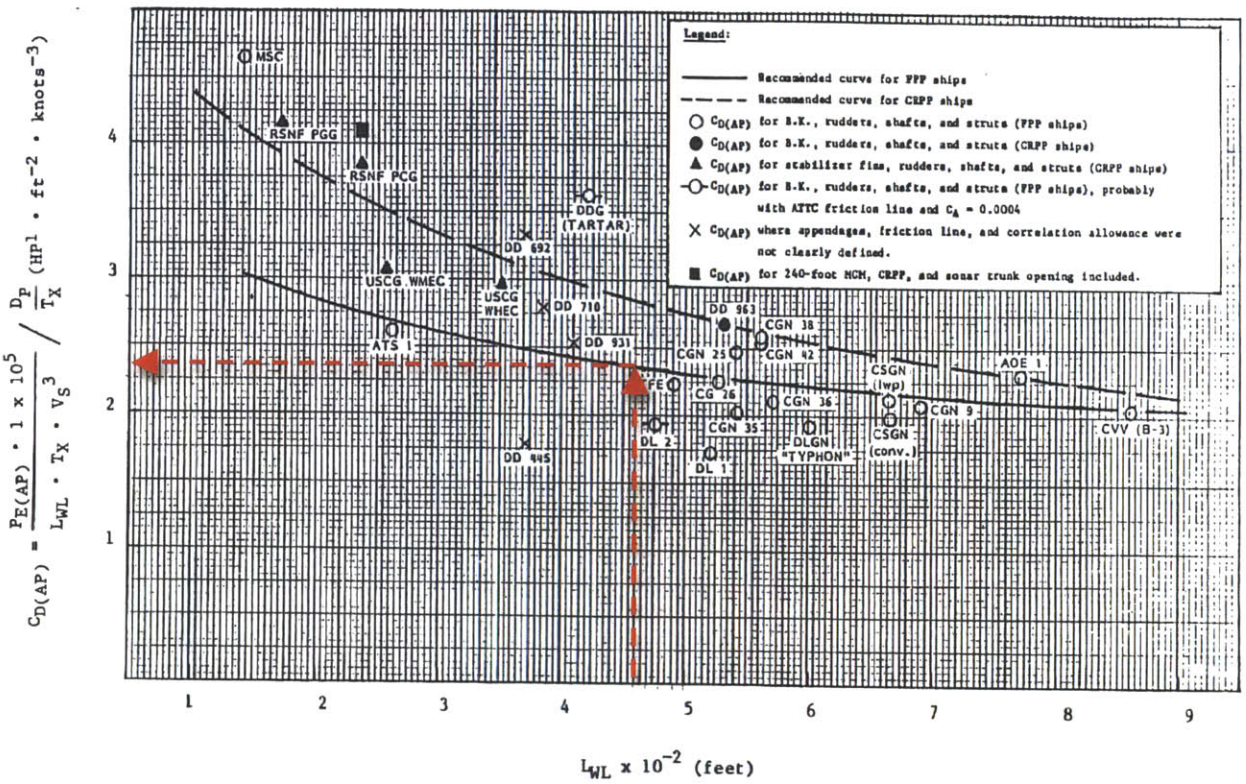

Figure 30 - Appendage Resistance Coefficient

Using Figure 30, for a ship with a fixed-pitch propeller and a length of 466 feet, the value for the appendage drag coefficient is 2.3.

3.3 Still-Air Drag

Still-air drag does not have an extensive effect on the ship's resistance, especially at lower speeds. Regardless, the DDS-051 suggests a formula to calculate the effective power of the air resistance:

$$P_{E(AA)} = \left(\frac{\rho_A}{2}\right) \cdot A_V \cdot V_S^3 \cdot C_{AA} \cdot \frac{1}{K_1}$$

where

ρ_A - is the density of air

A_V - is the above-water transverse area

C_{AA} - is the air drag coefficient (taken as 0.7 for destroyers or 0.75 for auxiliary ships)

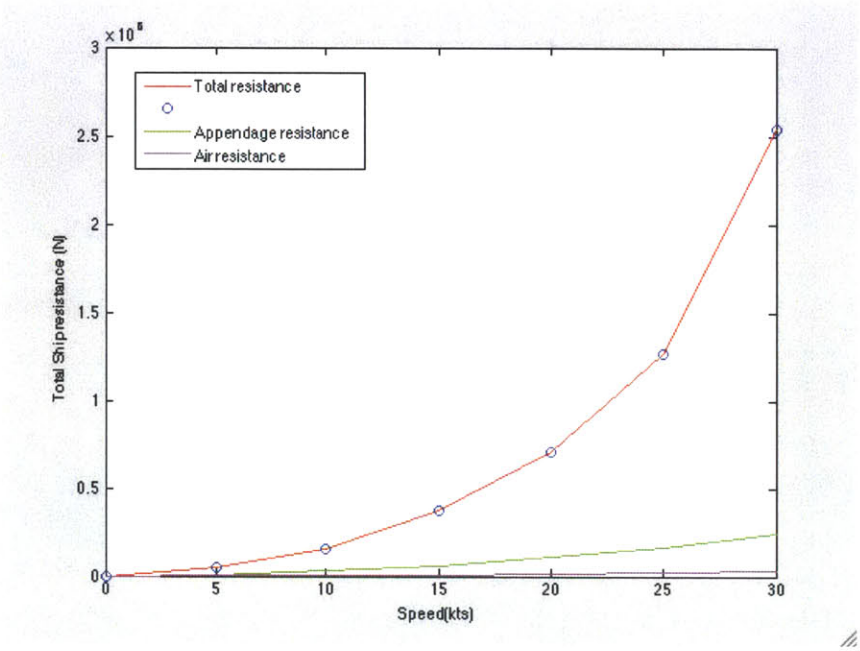

Figure 31 – **Full Scale Ship Resistance Force**

3.4 Total (Propulsion) Effective Power

The ship's total effective power at each speed is the power that the propellers will have to deliver into the water to overcome the resistance forces. It is common to calculate the effective power as (Zubaly, 1996):

$$EHP = R_S \cdot V_S$$

where R_S is the ship's total resistance (N) and V_S is the ship's speed.

The total EHP will have to include also the added power for appendages and air drag

$$EHP_t = EHP + P_{E(AP)} + P_{E(AA)}$$

The resistance force and the total effective power (EHP) are shown in Table 9.

Ship Speed (kts)	Fr	Bare hull resistance (N)	Appendage Resistance (N)	Air Drag (N)	Total Resistance (N)	EHP (HP)
10	0.13	0.12e+06	0.26e+05	0.37e+04	0.15e+06	1.08e+03
15	0.20	0.30e+06	0.59e+05	0.83e+04	3.71e+06	3.84e+03
20	0.28	0.58e+06	1.0e+05	1.48e+04	7.04e+06	9.72e+03
25	0.34	1.07e+06	1.6e+05	2.3e+04	1.26e+06	2.18e+04
30	0.41	2.27e+06	2.3e+05	3.3e+04	2.54e+06	5.26e+04

Table 8 – Total Resistance and Effective power

3.5 Total Thrust

Total thrust required is greater than the resistance calculated due to the thrust deduction coefficient *t*:

$$T = \frac{R_s}{(1-t)},$$

where T is the total thrust that the propeller is required to supply. The resistance of a self-propelled ship is different from that of a towed ship because the presence of an operating propeller changes the pressure distribution of the water around the hull, so the real thrust will be somewhat higher than the towed bare-hull thrust; *t*, the thrust deduction coefficient, accounts for this change.

Chapter 4 – Propeller Calculations

4.1 Propeller Load points

In the process of designing a new ship, the propeller design becomes a critical factor for testing feasibility of the design.

The interaction between the hull, propellers and engines should be carefully investigated and defined in a way that will produce an effective hull form that can accommodate engines and supporting machinery units with propellers that can efficiently deliver the power requested.

Generally speaking, increasing the propeller's diameter and decreasing the rotational velocity will produce higher propeller efficiency. Since the hull's shape and propeller proximity usually limit the allowable size of the propeller, the efficiency of the propeller is relatively low (around 70% at optimal conditions).

It would be possible to design a new propeller for the ship using software such as MIT's OpenProp, an open source propeller design tool (Kimball and Epps 2010); however, this is beyond the scope of the current project. For simplicity purposes, the propeller that was

Figure 32 – DDG-51 propellers (Jansengineering, 2009)

selected for the calculation was the same propeller that was used for the self-propulsion tow tank experiments. The characteristic parameters of the propellers were taken from the self-propulsion test report (Borla 1984).

The propellers used for the tests were from series 4876 and 4877 (Borla 1984). The full-scale diameter was set to be 5.18 meters (17 feet), which is the same size that is installed on the DDG-51 (Kravitz 2011), shown in Figure 33.

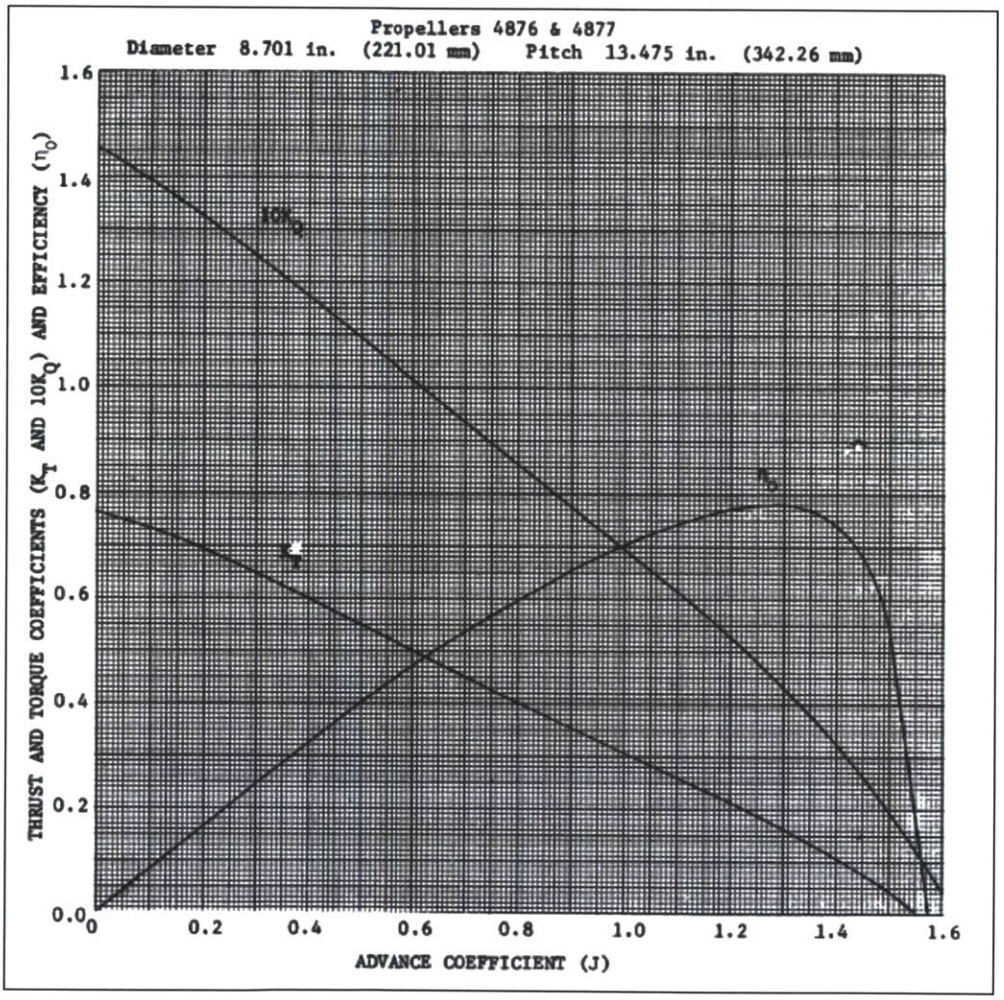

Figure 33 – 4876/4877 Propeller parameters, (Borla 1984)

The following coefficients are commonly used in propeller design (Woud and Stapersma, 2008):

Advance coefficient: $$J = \frac{V_S}{n \cdot D_P}$$

Thrust coefficient: $$C_T = \frac{K_T}{8 \cdot J^2 \cdot \pi} = \frac{T}{\frac{1}{2} \cdot \rho \cdot \pi \cdot V_a^2 \cdot R_P^2}$$

Torque coefficient: $$C_Q = \frac{K_Q}{16 \cdot J^2 \cdot \pi} = \frac{Q}{\frac{1}{2} \cdot \rho \cdot \pi \cdot V_a^2 \cdot R_P^3},$$

where V_S is ship speed, n is propeller rotation rate, D_P is propeller diameter, T is thrust developed at the corresponding advance coefficient, ρ is water density, $V_a = V_s(1 - w)$ is the mean speed of the wake the propeller encounters, w is the wake fraction which accounts for the variation in speed of inflow to the propeller, R_P is the propeller radius, and Q is the torque. Since V_S, R_P, and T are already known, J and n can be calculated for the desired speeds and K_T, K_Q and η_0 can be determined using Figure 33. The results for the full-scale ship are presented in Table 10.

Speed (kts)	Advance Ratio (J)	K_T	K_Q	η_0	n(RPM)
0	-	-	-		-
5	1.187	0.218	0.0538	0.768	25.09
10	1.256	0.184	0.0474	0.778	47.41
15	1.244	0.190	0.0486	0.777	71.83
20	1.228	0.198	0.0500	0.775	96.98
25	1.194	0.215	0.0531	0.770	124.68
30	1.106	0.257	0.0609	0.745	161.59

Table 9 – Propeller parameters results

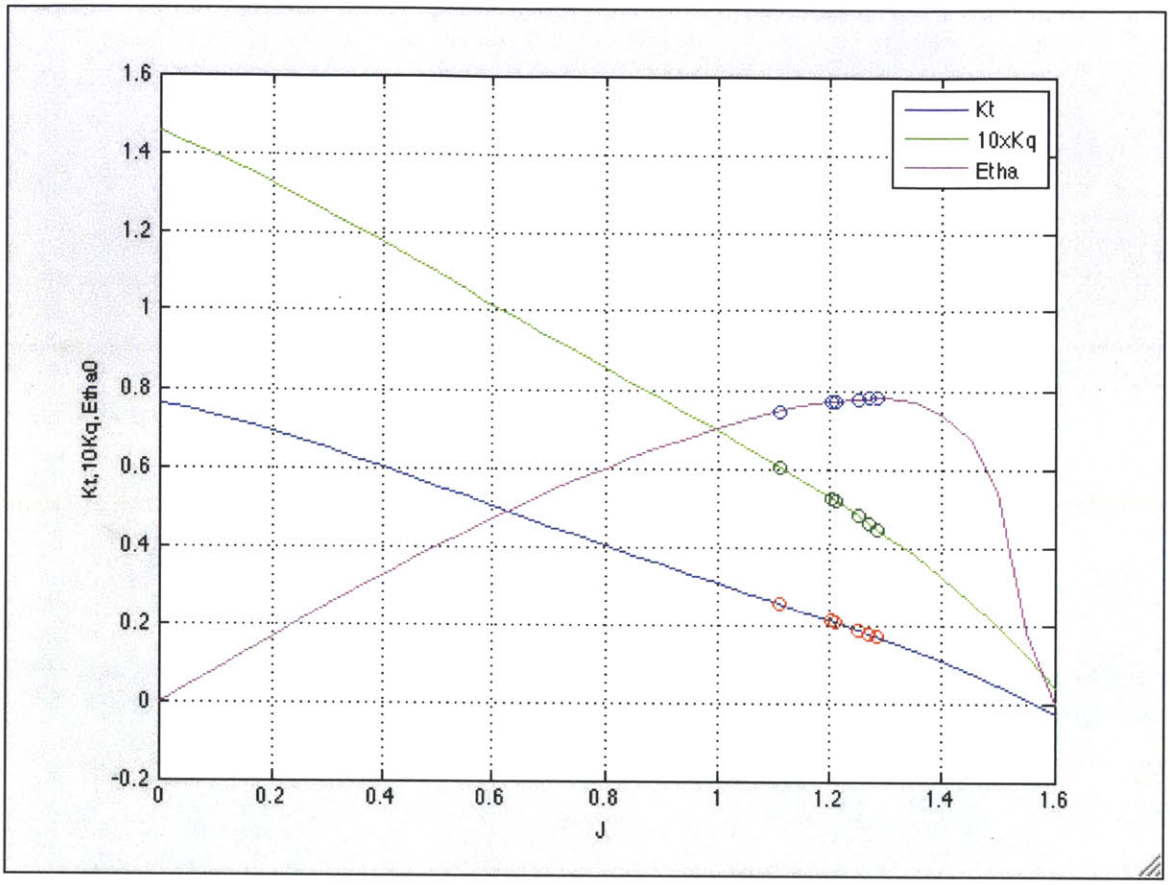

Figure 34 – Points of interest on propeller curves

Given J allows the calculation of K_Q and the propeller rotational velocity (revolutions per minute) so the torque (Q) can be calculated by:

$$Q = K_Q \cdot \rho \cdot n^2 \cdot D_P^5$$

And the power that needs to be produced:

$$P_P = 2 \cdot \pi \cdot n \cdot Q \qquad \text{(i)}$$

Using the resistance values from Table 9 and the propeller speeds from Table 10, we use Equation (i) to find the required propeller power. Assuming the shaft transmission efficiency is equal to 1, this is the power required as the output of the propulsion motor. Results are listed in Table 11.

Speed (kts)	n(RPM)	$P_P x10^4$ (HP)
0	-	-
5	24.76	0.0246
10	46.41	0.1462
15	70.43	0.5206
20	95.28	1.3193
25	122.98	2.9782
30	160.89	7.4294

Table 10 – Power delivered by propellers

4.3 Cavitation

Fitting a propeller to the ship is a complicated process that takes many factors into account:

a. Hull clearance: Propeller blade tips should have a sufficient clearance from the hull above.
b. Propeller Clearance: If the ship has more than one shaft, the designer must make sure that the distance between the shafts and propellers will not create any interaction, and disturbance on the propellers.
c. Cavitation: At higher speed of rotation, back cavitation may occur on the blades and create few unwanted phenomenon: 1. Pitting the blade – the collapse of the boiled pressurized water bubble can cause a substantial damage to the blade surface. 2. Thrust breakoff – a degradation in the propeller performance.

Since the design and optimization of a propeller are not within the scope of this work, calculating and presenting the cavitation behavior of the propeller in different speeds as a parameter for comparison and evaluation is suggested.

A very common criterion to compare propellers from a cavitation point of view is the Burrill curves as presented in many Naval Architecture texts. The curves are a

logarithmic representation of empiric parametric characteristics of the propeller, and present lines of constant blade back cavitation, as can be seen in Figure 35:

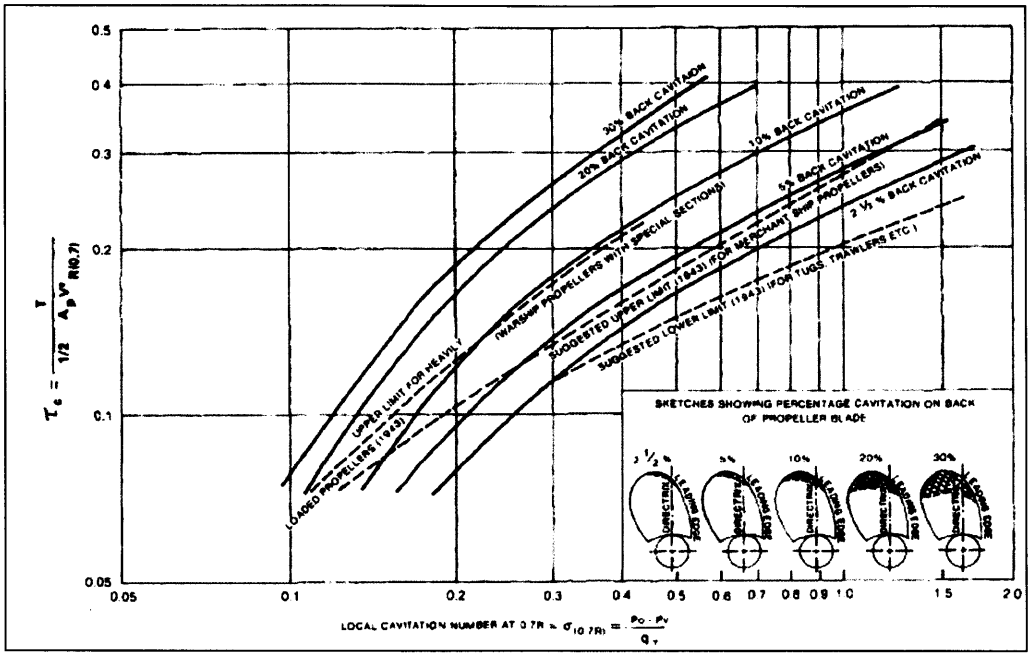

Figure 35 – Burrill Curves for Cavitation (Burrill, 1962)

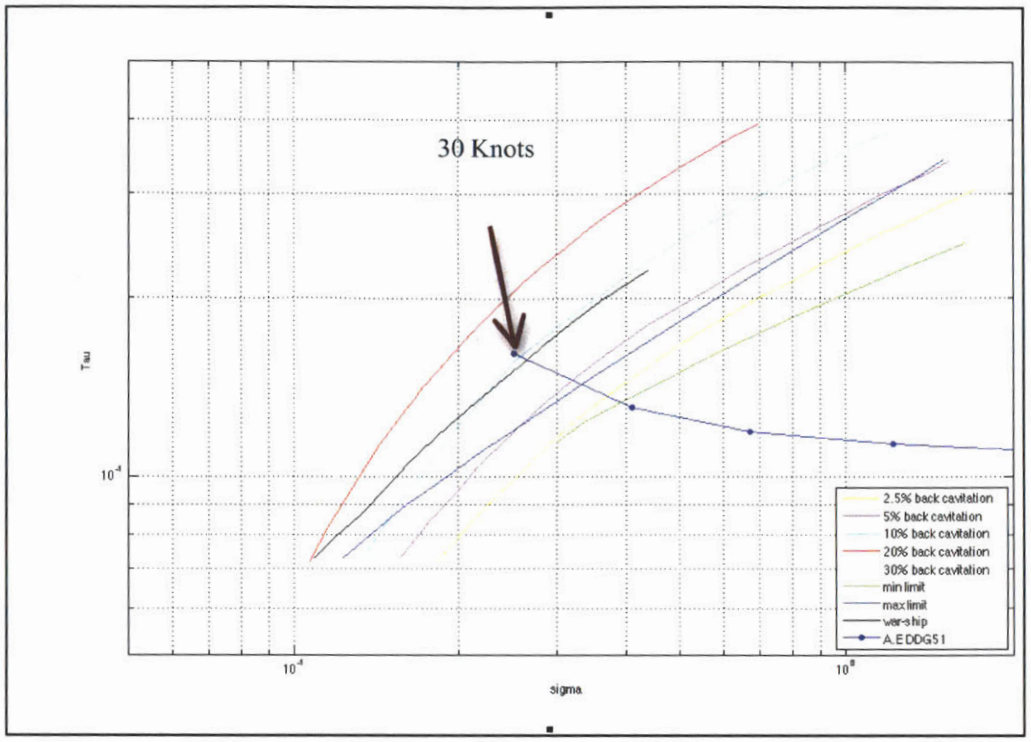

Figure 36 – Burrill Curves for Cavitation with AE.DDG51

It is clear that for the chosen propeller, which is not optimized for the hull, to expect that more than 10% of the blade will be covered by back cavitation. Lower speeds seem to be well below the line of the 2.5% and less.

It is also noticeable that the line that corresponds to naval warships is very close to the 10% back cavitation line, which confirms that the results are reasonable.

The influence of the cavitation on the performance (Thrust breakdown) should be small and can be calculated as part of a future development of this work, as suggested in the "Future Research" chapter.

Chapter 5 – Drive Train and Power

5.1 Machinery Configuration

The DDG51 operated by the US Navy has a mechanical drive train consisting of 4 LM-2500 gas turbines as prime movers (with a mechanical reduction gear box) and 3 Allison (AL501-K34) Gas Turbine generators for all ship service loads as shown in Figure 37.

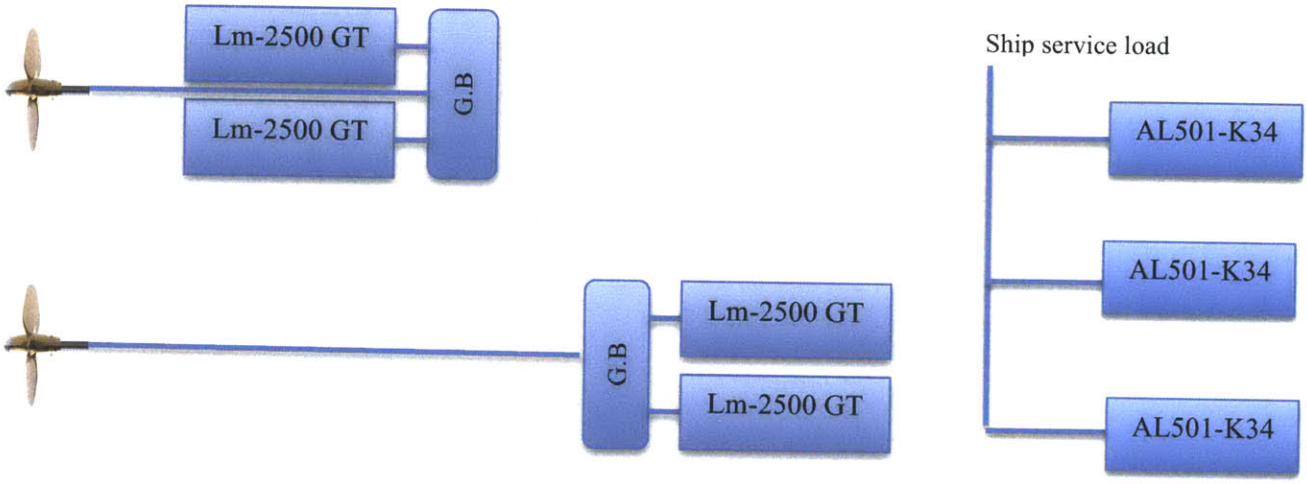

Figure 37 – Original DDG51 Drive Train

For this project, we assume an electric-drive ship with the propulsion and ship service load supplied by 4 LM-2500 gas turbine generators via a single electrical distribution system as shown in Figure 38.

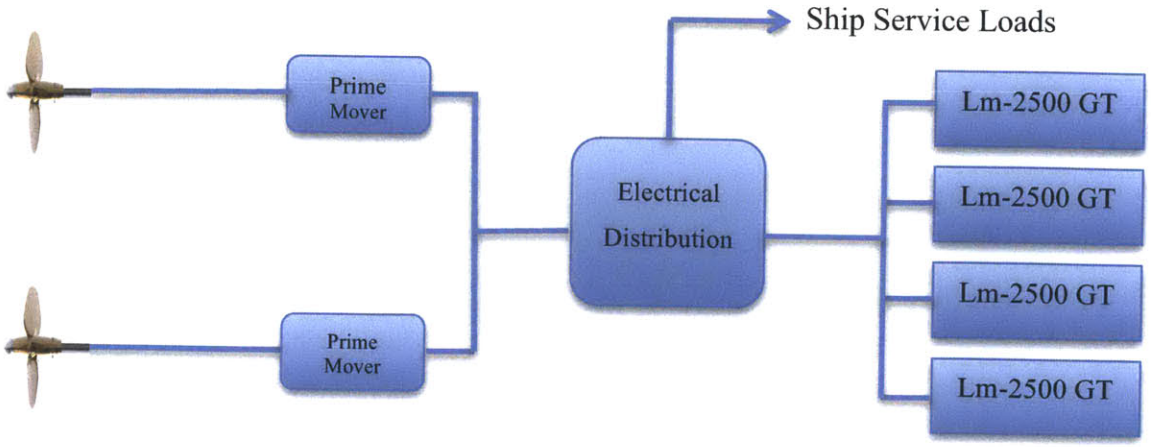

Figure 38 – Electric Drive DDG51 Drive Train

5.2 Total Engine Brake Power Calculation

Fuel consumption for an engine (gas turbine) is a function of the power it produces and the rotational speed of its shaft (RPM). Chapters 2 and 3 show the methodology used for finding the thrust required for a given speed, and Chapter 4 calculates the power that is needed to be delivered to the propeller to create this thrust. This chapter will discuss the methodology to calculate the total brake power that the engines deliver.

5.2.1 Operational Assumptions

Naval ships operate at various conditions during their service time, and even during a single mission. For example, operating in peacetime, battle condition, or at anchor will drastically change the equipment that is in use and the power demands of that equipment. For this project, we use the following five primary operational conditions:

a. Shore power – The ship is moored pierside, connected to a base utility power grid. At this condition, the generators produce none of the power for the ship's systems.

b. Anchor – The ship is at sea, but not moving, so the power produced by the generators is used for ship service loads and auxiliary systems only. None of the power is used for propulsion.

c. Peacetime Cruise – Power is produced for propulsion (speed dependent) and for basic ship service loads only.

d. Wartime Cruise – Power is produced for propulsion (speed dependent) and ship service loads, with fully functional weapon and defense systems, prepared to be activated at any given time.

e. Battle – Power is produced for propulsion (speed dependent) and ship service loads with all weapons and defense systems operating. Power generation is in a high-redundancy configuration so all generators are operating regardless of the power required.

To meet the power requirements of the different operational conditions at various speeds, the number of gas turbine generators in use must be selected. When a ship has multiple

shafts and multiple generators, a large number of combinations for operating the ships machinery can be created that would satisfy the power requirements. Some will be more efficient than others, and sometimes less efficient configurations will be chosen for operational considerations such as redundancy, engine hour limits, and others.

We make the following assumptions for our notional electric-drive destroyer:

a. No trailing shaft condition - both shafts are active at all times. This assumption is made for an electric-drive ship since any generator can deliver power to both electric motors with relatively low losses. This assumption will not be valid for a mechanical drive train in which a gas turbine is directly connected to only a single shaft, thus placing the engine load in an inefficient range for low speeds.
b. All generators are connected, and can deliver power to any electric motor.
c. While operating, all of the generators on line carry the same load (equal power is produced by each generator).

5.2.2 Operational Machinery Configurations

From the assumptions above, the machinery operational matrix was created, defining the number of generators that are operated for each of the operational condition and ship speed configurations as shown in Table 11.

Speed(kts)	Shore Pwr	Anchor	Peacetime Cruise	Wartime Cruise	Battle
0	0	1	1	2	4
5	0	0	1	2	4
10	0	0	1	2	4
15	0	0	1	2	4
20	0	0	1	2	4
25	0	0	2	3	4
30	0	0	4	4	4

Table 11 – Machinery configuration

The data was assumed for the calculations only. It is not correlated to any real documented machinery operational data, and can be changed easily in the Matlab code for future calculations.

5.2.3 Propulsion Power

The propulsion power is the portion of power that is used for moving the ship through the water. The thrust is created by electric power delivered to the electric motor, which rotates the shaft and propeller at the proper rotational speed.

In Chapters 2 through 4, the required thrust for each ship speed and the correlated rotational speed for the shaft and propeller were calculated. The total power required from the gas turbines for propulsion only is calculated by the power delivered from the propeller to the water, divided by the efficiencies up the line to the gas turbine. These efficiencies include the motor and motor drive, the transmission system, the generator and rectifier if applicable, and the gas turbine.

The electric motor efficiency, $\eta_{pmm,}$ is a function of the power delivered to the propeller. We use the generic values given by DDS-200-1 (NAVSEA 2011) and interpolated into Table 12.

Speed(kts)	Shore Pwr	Anchor	Peacetime Cruise	Wartime Cruise	Battle
0	N/A	N/A	0.84	0.84	0.84
5	N/A	N/A	0.85	0.85	0.85
10	N/A	N/A	0.88	0.88	0.88
15	N/A	N/A	0.89	0.89	0.89
20	N/A	N/A	0.91	0.91	0.91
25	N/A	N/A	0.94	0.94	0.94
30	N/A	N/A	0.94	0.94	0.94

Table 12 – Electric Motor Efficiency

Dividing the value of TBP(HP) by the number of running engines (Table 11) produces the total brake power for propulsion loaded on each running engine. The results are gathered into Table 13.

Speed (kts)	Shore Pwr	Anchor	Peacetime Cruise	Wartime Cruise	Battle
0	0	0	0	0	0
5	0	0	0.0259	0.0129	0.0065
10	0	0	0.1539	0.0769	0.0385
15	0	0	0.5482	0.2741	0.1371
20	0	0	1.3887	0.6943	0.3472
25	0	0	1.5675	1.0450	0.7837
30	0	0	1.9551	1.9551	1.9551

Table 13 – Propulsion power per engine online (x10^4 HP)

5.2.4 Ship Systems Electric Load

The ship systems electric load is mostly utilized for weapon systems operation and auxiliary systems.

It is assumed here that the ship loads do not change with ship's speed, only with battle condition; thus each operational state (Battle, Wartime Cruise, etc.) has a characteristic load that is constant with speed. This load is shown in Table 14.

	Shore Pwr	Anchor	Peacetime Cruise	Wartime Cruise	Battle
Ship Electric Load (HP)	0	6000	11000	13000	14000

Table 14 – Ship Electric Load (HP)

Detailed analysis of the electrical distribution system is beyond the scope of this project. To obtain an appropriate efficiency for distribution of power to the ship service loads, we used the notional electrical distribution systems proposed for use in the Electric Ship Research and Development Consortium (ESRDC 2011) and the associated efficiencies for specific pieces of equipment as determined during the analysis for (Chioccio, 2011). We assumed a constant efficiency for the electrical distribution system of $\eta_{mvdc} = 0.94$

for a medium voltage DC (MVDC) distribution system and $\eta_{mvac} = 0.98$ for a medium voltage AC (MVAC) distribution system. This calculation is shown in Appendix B.

5.2.5 Total Brake Power

The total brake power is the power produced by the engines, before being used, transformed or distributed to other systems/consumers, and is usually referred to as BHP (Brake Horsepower) when using horsepower units.

From all power calculations through the drive train components, the brake power is the last one calculated, summing the ship's service electric loads (divided by the electric load efficiencies) and the propulsion power load (divided by the electric/mechanical efficiencies).

The Total Brake power is calculated as follows:

$$Total\ Brake\ Power(MVDC) = Propulsion\ brake\ power + \frac{Total\ ship\ load\ power}{\eta_{mvdc}}$$

$$Total\ Brake\ Power(MVAC) = Propulsion\ brake\ power + \frac{Total\ ship\ load\ power}{\eta_{mvac}}$$

Note that the efficiency for the propulsion power is the same for MVDC and MVAC. This is because the propulsion motors are driven by a variable-frequency motor drive. In the MVAC system, a rectifier is required prior to the motor drive; in the MVDC system, the power is rectified before transmission, so the efficiencies are the same. This rectifier efficiency is included in the motor efficiency described above. While there is some slight difference in the cable losses in the transmission of the power from the generators to the motors, the difference is negligible for this study.

The results for MVDC are shown in Table 15.

Speed (kts)	Shore Pwr	Anchor	Peacetime Cruise	Wartime Cruise	Battle
0	0	0.638	1.170	1.383	1.489
5	0	0	1.196	1.408	1.515
10	0	0	1.324	1.536	1.643
15	0	0	1.718	1.931	2.037
20	0	0	2.558	2.771	2.878
25	0	0	4.305	4.518	4.624
30	0	0	8.990	9.203	9.309

Table 15 – Propulsion power MVDC(x10^4 HP)

The results for MVAC are shown in Table 16.

Speed (kts)	Shore Pwr	Anchor	Peacetime Cruise	Wartime Cruise	Battle
0	0	0.612	1.122	1.326	1.1.428
5	0	0	1.148	1.352	1.454
10	0	0	1.276	1.480	1.582
15	0	0	1.670	1.874	1.976
20	0	0	2.511	2.715	2.817
25	0	0	4.257	4.461	4.563
30	0	0	8.942	9.146	9.249

Table 16 – Propulsion power MVAC(x10^4 HP)

Chapter 6 – Fuel Consumption Prediction

Fuel consumption prediction for an engine, and especially for a gas-turbine engine, is a complicated process that needs to take many factors into account in order to get a good estimation.

The fuel consumption of a gas turbine is a function of the power, the RPM, the inlet temperature of the air, and more. High temperatures may lower the maximum power of the turbine, and change its fuel consumption. For the sake of this calculation, and without data to describe the ambient temperatures the ship might operate in, it was decided to calculate for the optimal conditions of $59°F$.

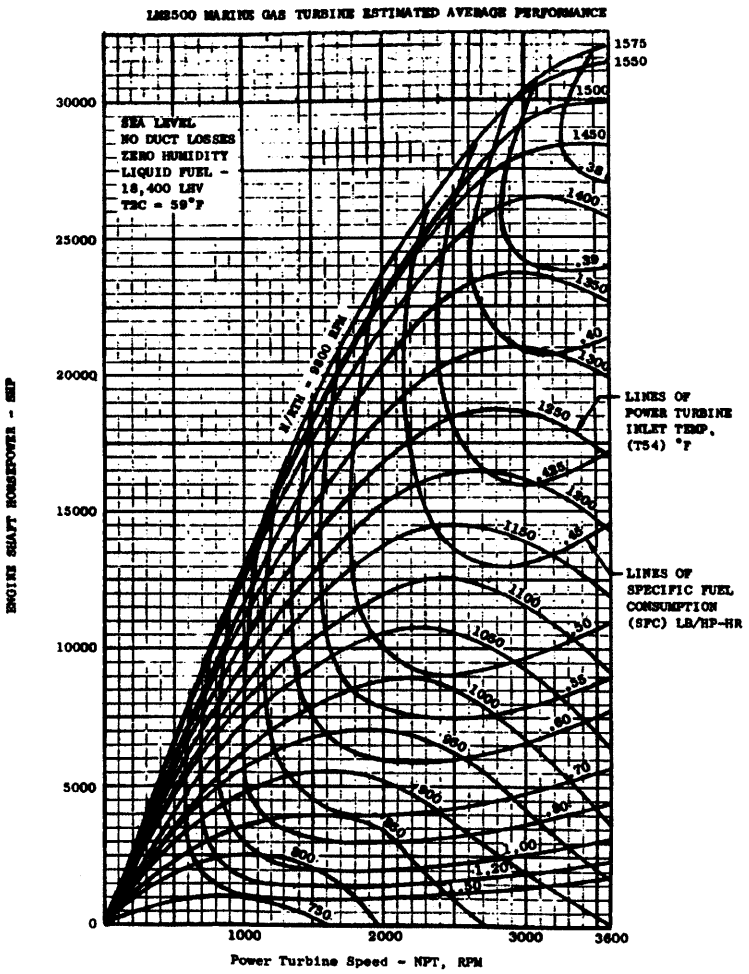

Figure 39 – LM2500 SFC Curves

The gas turbines, as described earlier in this report, were standard LM-2500 GT with the SFC (Specific Fuel Consumption) curve in Figure 39.

To produce AC power, the generator is operated at a constant speed of 3600 rpm. For a DC distribution system, the power is rectified immediately after being generated, so frequency can vary and the gas turbine can thus be operated at the most efficient speed for its load. Thus, interpolating Figure 39 for constant speed of 3600 rpm and for most efficient speed produces the SFC curves shown in Figure 40 for the MVAC and MVDC power distribution systems.

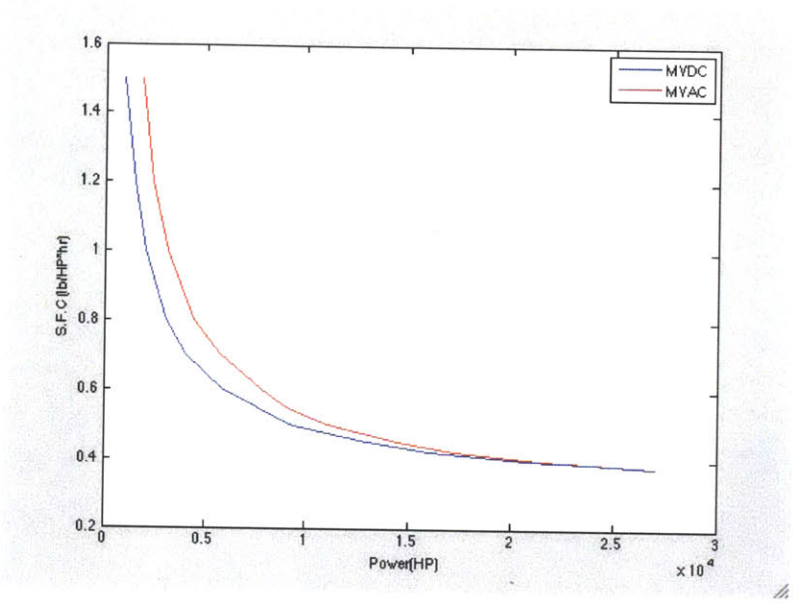

Figure 40 – MVDC and MVAC S.F.C curves

Figure 40 shows clearly, that for low power loads, MVDC will consume less fuel then MVAC. At high power loads (above 20,000HP per engine) the S.F.C will be the same since the RPM will get closer.

Table 17 and 18 show the specific fuel consumption values per engine hp-hour for the power requirements at each speed and battle condition for MVDC and MVAC respectively.

Speed (kts)	Shore Pwr	Anchor	Peacetime Cruise	Wartime Cruise	Battle
0	0	0.583	0.463	0.567	0.724
5	0	0	0.460	0.563	0.717
10	0	0	0.446	0.542	0.690
15	0	0	0.414	0.485	0.627
20	0	0	0.380	0.436	0.551
25	0	0	0.394	0.427	0.459
30	0	0	0.390	0.388	0.387

Table 17 – MVDC S.F.C (lb per hp-hour)

Speed (kts)	Shore Pwr	Anchor	Peacetime Cruise	Wartime Cruise	Battle
0	0	0.678	0.497	0.654	0.926
5	0	0	0.491	0.647	0.913
10	0	0	0.469	0.616	0.858
15	0	0	0.424	0.530	0.744
20	0	0	0.382	0.454	0.622
25	0	0	0.396	0.439	0.485
30	0	0	0.391	0.389	0.388

Table 18 – MVAC S.F.C (lb per hp-hour)

It is clear to see from Figure 40 and Tables 17 and 18 that when engines are highly loaded, the specific fuel consumption in MVDC is similar to MVAC, while at lower loading conditions, the difference is significant. Table 19 compares the SFC for MVDC and MVAC as a percentage of increased SFC from MVDC to MVAC.

Speed (kts)	Shore Pwr	Anchor	Peacetime Cruise	Wartime Cruise	Battle
0	N/A	16%	7.2%	15%	27.8%

5	N/A	N/A	6.8%	14.8%	27.2%
10	N/A	N/A	5.3%	13.7%	24.3%
15	N/A	N/A	2.4%	9.2%	18.6%
20	N/A	N/A	0.4%	4.0%	13.0%
25	N/A	N/A	0.57%	2.9%	5.5%
30	N/A	N/A	0.23%	0.2%	0.19%

Table 19 – SFC percent difference between MVDC and MVAC

Since the number of working engines for each operational configuration was determined arbitrarily (without any formal Navy document to confirm) the numbers for the real ship will probably be different. The trend however is clear – MVDC is using the engines more efficiently at lower loads.

Chapter 7 – Tankage

The formal Navy document for tankage calculation is the DDS-200 (NAVSEA, 2011). The document suggests different methods for calculation of required fuel tank capacity. In this work we demonstrate the methodology for endurance fuel capacity calculation.

The document (DDS-200) suggests an operational profile for DDG-51 slightly different than the one we selected in earlier stages of the research. Since the methodology can be adapted to any operational profile, any ship, and any power management configuration, the tankage was calculated for the operational profile that was used so far.

The DDS-200 recommends calculating the amount of fuel required for three possible scenarios, and using the largest of the three results to size onboard storage tanks. The three scenarios include:

1. Range: Traveling at endurance speed for the ship's required range (we use 5000 nautical miles at 16 knots)
2. Surge to theatre: traveling at maximum sustained speed for a surge range (we use 2000 nautical miles at 30 knots)
3. Operational presence: conduct operations for a specified number of days without refueling (this requires a specific mission profile over a typical day)

Due to the difference in the operational profiles, this work did not include the Operational Presence calculation.

The results calculated for cases 1 and 2, for MVAC and MVDC are shown in Table 20.

	MVDC			MVAC		
	Peace time cruise	War time cruise	Battle	Peace time cruise	War time cruise	Battle
Endurance Tankage	1,336	1,656	2,166	1,318	1,689	2,398
Surge to theatre Tankage	1,294	1,317	1,328	1,290	1,312	1,322

Table 20 – Fuel Tankage (Meters tons)

With the assumption of Peace Time Cruise as the guiding condition for endurance tankage, the result will be 1,336 tons for MVDC and 1,318 for MVAC.

Chapter 8 – Annual Fuel Consumption

One important parameter, calculated for the ship's LCC (Life Cycle Cost) is the annual fuel usage – the tonnage of fuel used by one ship in one year (of active service, not including repairs, or docked periods).

The goal is to have a gross assessment of the annual fuel usage, which can be used to compare different ships or different variants.

The annual fuel consumption is calculated using the following equation:

$[Operational\ Profile] \cdot [S.F.C] \cdot [\text{Power}] \cdot [Total\ Time] = Annual\ Fuel\ Usage,$

where "Operational Profile" is the percentage of time spent in a typical year at each speed/condition, SFC is the specific fuel consumption (fuel consumed per hour of operations per unit of power) of all online gas turbine generators at the power level required for that speed/condition, "Power" is the power required to meet the speed and battle condition, and "Total Time" is one year. Every point on the operational profile has a correlated value of specific fuel consumption (as seen in tables 17 and 18).

For MVDC:

$$\Sigma\left\{\begin{bmatrix}53 & 1.58 & 0 & 0 & 0\\ 0 & 0 & 6.8 & 5.1 & 0.1\\ 0 & 0 & 4.7 & 3.6 & 0.07\\ 0 & 0 & 6.4 & 4.8 & 0.1\\ 0 & 0 & 6.0 & 4.5 & 0.1\\ 0 & 0 & 1.5 & 1.1 & 0.02\\ 0 & 0 & 0.13 & 0.1 & 0\end{bmatrix} \cdot \begin{bmatrix}0 & 1.58 & 0.463 & 0.567 & 0.724\\ 0 & 0 & 0.460 & 0.563 & 0.717\\ 0 & 0 & 0.446 & 0.542 & 0.690\\ 0 & 0 & 0.414 & 0.485 & 0.627\\ 0 & 0 & 0.380 & 0.436 & 0.551\\ 0 & 0 & 0.394 & 0.427 & 0.459\\ 0 & 0 & 0.390 & 0.388 & 0.387\end{bmatrix} \cdot \begin{bmatrix}0 & 0.638 & 1.17 & 1.38 & 1.48\\ 0 & 0 & 1.19 & 1.40 & 1.51\\ 0 & 0 & 1.32 & 1.53 & 1.64\\ 0 & 0 & 1.71 & 1.93 & 2.03\\ 0 & 0 & 2.55 & 2.77 & 2.87\\ 0 & 0 & 4.30 & 4.51 & 4.62\\ 0 & 0 & 8.99 & 9.20 & 9.30\end{bmatrix} \cdot \mathbf{10^4 \cdot 365 \cdot 24}\right\} = \mathbf{16,746\ Tons}$$

For MVAC, applying the same process described above produced 17,275 Tons.

Chapter 9 – Summary and Conclusions

The results for the methodology presented can be separated to 3 different aspects addressed below.

9.1. CFD case preparation:

- Star-CCM+© that was used for the resistance CFD calculation, was a very friendly platform to work with, even though some of the functions operate as "black box" which makes it harder to understand.

- The geometry file used for the hull has a critical importance for a successful process. A hull with bad properties may fail the process or impose wrong answers.

- A strong computer that allows parallel computing is essential for the speed of the process.

9.2. The CFD Calculation and Results:

- The average results for the resistance forces, generated with Star-CCM+©, seem accurate enough (compared to the towing tank results) to be used as the resistance predictor for the fuel consumption prediction methodology.

- For lower speeds (10 knots and lower) CFD might even be a more accurate prediction for the resistance then towing tank experiments. The towing tank report that was used as a reference (Olivieri,1991) proves low accuracy at low speeds.

- Despite the oscillation in the pressure force result, the average value was a good approximation. The occurrence of the oscillation was not fully investigated and will have to be revisited.

9.3. The Fuel Consumption Calculation:

- Figure 40 shows clearly a significant difference between MVDC and MVAC specific fuel consumption when the engines are running at low loads.

- Electrical production and transmission is more efficient for MVDC than MVAC and improved efficiencies can be seen for items such as variable frequency drives or variable speed pumps or fans; however, for this example ship, in-zone electrical loads are less efficient for MVDC because power is rectified then inverted by the distribution system, which is not required in MVAC. Due to this, fuel requirement calculations can show some interesting results. In our case, the annual fuel consumption is lower (more efficient) for the MVDC version, but onboard tankage is higher because the onboard tankage calculation is performed at a more efficient point in the SFC curve.

- Annual fuel usage includes only consuming fuel from the ships tanks for power and propulsion. But in 53% of the time, the ship is supplied with external power and its fuel consumption for the sake of the calculation herein, is assumed to be zero. If the calculation is done for LCC, it is important to include the cost of power consumed at all times.

- The Matlab code permits changes in the number of engines that are online for a given speed and battle condition combination. It would be possible to use this code for an optimization process to adjust the number of engines online to ensure that the engines are loaded properly when taking operational condition into consideration. It is also important to note that the operational profile has a significant effect on the overall efficiency results.

Chapter 10 – Future Research

From the research done in the process of developing the methodology described in this report, a few ideas for further research came up and may contribute to a better understanding of the results:

1. Oscillating force results: From all the CFD runs, it was clear that the pressure force calculated in the program is disturbed by some perturbation/numeric error that creates an oscillatory behavior in the water. It is highly recommended to further discuss and search for the reason for it. Then, it will be useful to eliminate or shrink the phenomenon. Changing the mesh and the size of the domain seems like the first step that needs to be done for better understanding of the case.
2. Free Hull in Pitch and Heave: The cases that were tested in the scope of this report were predefined to be fixed in space, with the trim angle and sinkage taken from the average values of the tow tank experiments. As was observed in the results during the run, it might be interesting to check further the proximity of the CFD prediction for heave and pitch motion, relative to the tow tank experiment.
3. Full Scale Hull: Since one basic goal of this research was to prove that the CFD program could predict resistance accurately for use in the fuel prediction methodology, the selected hull was a model size hull (with existing data base to compare). Further research should run a full-scale hull and determine the accuracy of such prediction.
4. Cavitation Thrust Breakdown: Using the Burrill cavitation criteria shows some cavitation at high speeds. A future research can calculate the degradation of thrust due to the cavitation.
5. Different Hull Type: It might be also interesting to see how accurate a CFD prediction can be for different hull types such as Catamaran, SWATH, Planning hull and more.

References

- Robert B. Zubaly, "Applied Naval Architecture", 1996. Cornell Maritime Press, Inc.

- Lars Larsson and Hoyte C. Raven, "Ship Resistance and Flow", 2010, Principles of Naval Architecture series.

- Althea de Souza, "How to understand Computational Fluid Dynamics Jargon", 2005 NAEMS Ltd.

- NAVSEA, DDS-051-1, "Prediction of smooth-water powering performance for surface displacement ship", 15 May 1984.

- NAVSEA, DDS-200-1 REV1, "Calculation of Surface Ship Endurance Fuel Requirements", 04 October 2011

- Gary Borda, "Resistance, powering and optimum rudder angle D.W. Taylor Experiments on a 142m DDG-51", January 1984.

- J.S.Chalfant and C. Chryssostomidis, "Toward the Development of an Integrated Electric Ship Evaluation Tool", 2009.

- R.W. Kimball and B.P. Epps, "OpenProp v2.4 propeller/turbine design code," http://openprop.mit.edu, 2010.

- ITTC-Recommended Procedure: Testing and Extrapolation Methods, 7.5-02-03-01.1. 2002.

- Tim Chiocchio, Julie Chalfant, Steve Pekarek, Mike Mazzola, Mischa Steurer, John Herbst, "Size and Weight Comparison of Notional Systems", 29 July, 2011.

- ESRDC, "Documentation for Notional Baseline System Models, Version 0.31, DRAFT", September 2011.

Appendix A – Matlab Code

```
% FUEL CONSUMPTION PREDICTION METHODOLOGY FOR EARLY STAGES OF NAVAL
SHIP DESIGN
%
%                                        __
%                                     ___||_      _
%                                 ____/______\___/|\____
%--_____---_______---_______\   Eran Gheriani       |___---___---____
%==_______===_______===_______\_____________________|___===___===____
%--_________---_______---_______-----_______-----_______---_____-----__
%%%%%%%%%%%%%%%%%%%%%%%%%%%%%%%%%%%%%%%%%%%%%%%%%%%%%%%%%%%%%%%%%%%%%%%
%%%%%%%%%%
```

```
%Main file
clear all
close all
clc

%Constants:

Lm=5.72;                %Length of model (m)
Tm=0.248;               %Draft of model (m)
Am=4.786;               %Underwater are of model (m^2)
Bm=0.76;                %Beam of model (m)

Gama=24.824;            %Scale of model

Ls=Lm*Gama;             %Length of ship (m)
Bs=Bm*Gama;             %Beam of ship (m)
Ts=Tm*Gama;             %Draft of ship (m)
As=Am*Gama^2;           %underwater area of ship (m^2)
Dp=5.18;                %propeller diameter
z=2;                    %number of shafts
ne=4;                   %number of gas turbine
in2m=0.0254;

rho_sw=1025;            %sea water density (kg/m^3)
rho_fw=997;             %tow tank water density (kg/m^3)

Temp=25;                %water temperature (C)
Rho_air=1;              %Air density (kg/m^3)
A_us=400;               %Upper structor front projected area (m^2)


%Viscousity formula from ITTC 1978 (doc 7.5-02)

ni_fw=((0.585e-3*(Temp-12)-0.03361)*(Temp-12)+1.235)*10e-6;
%kinematic viscousity of fresh water
ni_sw=((0.659e-3*(Temp-10)-0.05076)*(Temp-1)+1.7688)*10e-6;
%kinematic viscousity of Sea water

g=9.81;                 %gravity acceleration m/sec^2

kts2ms=0.51444;         %convert from knots to m/s
```

```
hp2kw=1/0.745;
%lb2kg=0.45359;          %Mult factor to convert from lb to kg

time=365*24;             %Hours per year

Vs_kts=[0 5 10 15 20 25 30];          %ship speed in knots
Vs=Vs_kts*kts2ms;                     %convert ship speeds to m/s
Vk=10;                                %wind velocity-assumed constant
(m/s)

% Enter experiment data results:

Vm=[0 0.51 1.03 1.54 2.097 2.54 3.071];          %Speeds at tow tank
(m/s)
Rfm=[0 2 9 18 30 43 64];                         %tow tank Friction
force (N)
Rpm=[0 1 1.4 5 13 30 90];                        %tow tank pressure
force (N)
Rtm=Rfm+Rpm;                                     %tow tank total force
(N)

%figure(1)
%plot(Vm, Rtm)

Fr_t=Vm/sqrt(g*Lm);

%_____________________________________________________________________%

%Calculating the Resistance dimensionless coefficients:

Vs_ref=[4 8 12 16 20 24 28 32];
%reference speed from other report
R_ref=[26127.5 94773 201843.4 369106.7 652573.9 1001668.6 1756114.3
3060610.3];     %reference Resistance force from other report

L_Vm=length(Vm);
for i=1:1:L_Vm

Cf_m(i)=Rfm(i)/(0.5*rho_fw*Am*Vm(i)^2);          %Calculating frictional
resistance coeff
Cp_m(i)=Rpm(i)/(0.5*rho_fw*Am*Vm(i)^2);          %Calculating pressure
resistance coeff

end

Re_m=Vm*Lm/ni_fw;                                %Model Reynolds number
Re_s=Vs*Ls/ni_sw;                                %Ship Reynolds number

%Calculating resistance coefficients for the ship

for i=1:1:L_Vm
    Cf_s(i)=0.075/(log10(Re_s(i))-2)^2;
    Cp_s(i)=Cp_m(i);
    Ca_s(i)=0.0005;
    Ct_s(i)=Cf_s(i)+Cp_s(i)+Ca_s(i);
```

```
    Rt_s(i)=0.5*rho_sw*As*Vs(i)^2*Ct_s(i);       %Total bare-hull
resistance force (N)

end


%Calculating Air resistance by DDS-051-1

R_air=0.7*(Rho_air/2)*A_us.*Vs.^2;

%Calculate Hull appendages by DDS-051-1


%Calculat TOTAL ship resistance:
R_app=142*5.18*Vs.^2*2.3*10.76*7.36*745/100000;
%Appendages power calculation
R_compare=R_app./Rt_s;
R_total=Rt_s+R_air+R_app;
R_total(1)=0;

figure(1)
plot(Vs_kts,R_total,'r')
xlabel('Speed(kts)')
ylabel('Total Ship resistance (N)')
hold on
scatter(Vs_kts,R_total)
plot(Vs_kts,R_app,'g')
plot(Vs_kts,R_air,'m')
legend('Total resistance','','Appendage resistance','Air
resistance','Location','northwest')

for i=1:1:length(Vs)
    EHP(i)=R_total(i)*Vs(i)*1.341/(1000);  % total propulsion EHP in
HorsePower
end

figure(10)
scatter(Vs_kts,EHP,'b')
hold on
plot(Vs_kts,EHP,'r')
xlabel('speed(knots)')
ylabel('E.H.P(HP)')


%_____________________________________________________________________

%Efficiencies and propeller data:

etha_r=0.985;                                %from Julies paper or the
values vary from 0.935 to 0.950, i assumed constant
t=0.05;
w=0.015;
etha_h=(1-t)/(1-w);

N_GT=[0 1 1 2 4;0 0 1 2 4;0 0 1 2 4;0 0 1 2 4; 0 0 1 2 4;0 0 2 3 4;0 0
```

```
4 4 4];  %Total number of gas turbines on-line matrix

NS=[2 2 2 2 2 2 2];                                  %# of shafts
(1=trailing shaft,2=two shafts)

%Ne_t=N_GT_S1+N_GT_S2;


T=(1/(1-t))*(R_total);                          %T is the Total Thrust
created by propellers to move ship @ Vs

for i=1:1:length(Vs)
    T_S1(i)=T(i)/(NS(i));                       %T_S1 is the Thrust per
shaft assuming equal power on for two shafts
    T_S1(isnan(T_S1))=0;
end
T;
T_S1;
T./T_S1;
%Input - Propeller Kt,Kq,J from Experiment  prop 4876/4877

J=[0.0 0.05 0.1 0.15 0.2 0.25 0.3 0.35 0.4 0.45 0.5 0.55 0.6 0.65 0.7
0.75 0.8 0.85 0.9 0.95 1.00 1.05 1.1 1.15 1.2 1.25 1.3 1.35 1.4 1.45
1.5 1.55 1.6];
Kt=[0.7615 0.7475 0.7315 0.7130 0.6935 0.6715 0.6490 0.6255 0.6015
0.5765 0.5515 0.5265 0.5010 0.4760 0.4510 0.4265 0.4015 0.3775 0.3540
0.3300 0.3070 0.2835 0.2605 0.2365 0.2125 0.1875 0.1625 0.1355 0.1075
0.077 0.0445 0.009 -0.0295];
Kq=0.1*[1.457 1.426 1.3935 1.3595 1.324 1.288 1.251 1.2125 1.174 1.1345
1.095 1.056 1.015 0.975 0.935 0.8955 0.8555 0.8155 0.776 0.736 0.696
0.655 0.614 0.571 0.5265 0.4805 0.431 0.379 0.3225 0.2620 0.1955 0.1225
0.042];
etha_0=[0.0 0.042 0.084 0.125 0.167 0.207 0.248 0.287 0.326 0.364 0.401
0.436 0.471 0.505 0.537 0.569 0.598 0.627 0.653 0.678 0.702 0.724 0.743
0.759 0.771 0.778 0.780 0.769 0.74 0.678 0.543 0.181 0];
EA=47.722*in2m^2*Gama^2; %expanded area
PA=22324*Gama^2/1000000; %projected area
%Plotting Kt,Kq,etha_0 for the given propeller:

%Input - propeller Kt,Kq,J optional propeller 4119
%J=[0.5 0.7 0.833 0.9 1 1.1];
%Kt=[0.28 0.205 0.15 0.125 0.075 0.03];
%Kq=0.1*[0.46 0.36 0.28 0.24 0.18 0.11];
%etha_0=[0.4844 0.6344 0.7102 0.7460 0.6631 0.4775];


figure(3)
plot(J,Kt,'b')
hold on
plot(J,10*Kq,'g')
hold on
plot(J,etha_0,'m')
xlabel('J')
ylabel('Kt,10Kq,Etha0')
legend('Kt','10xKq','Etha')
grid on
```

```
for i=1:1:length(J)
    Ct(i)=Kt(i)*8/(J(i)^2*pi);
    Cq(i)=Kq(i)*16/(J(i)^2*pi);

end

% calculating Ct at ship speeds:
for i=1:1:length(Vs)
    Va(i)=Vs(i)*(1-w);
    Ct1(i)=T_S1(i)/(0.5*rho_sw*Va(i)^2*pi*(Dp/2)^2);
    Cq1(i)=T_S1(i)/(0.5*rho_sw*Va(i)^2*pi*(Dp/2)^3);
end

% Calculating J at points of interest (interpolation)
Js=pchip(Ct,J,Ct1);

% Plotting the points of interest on the Ct1(J) curve
figure(4)
plot(J,Ct)
xlabel('J')
ylabel('Ct')
hold on
scatter(Js,Ct1)
set(gca,'ylim',[0 10])
grid on

% Claculating the RPM

for i=1:1:length(Js)
    n(i)=Vs(i)/(Js(i)*Dp);
end

rpm=n*60;                                    %from rotations per second
to rpm
Kq1=interp1(J,Kq,Js);
Kt1=interp1(J,Kt,Js);
%Find open water efficiencty for speeds of interest:
etha_00=pchip(J,etha_0,Js);


figure(3)
hold on
scatter(Js,etha_00)
hold on
scatter(Js,10*Kq1)
hold on
scatter(Js,Kt1)
%_____
____
%CALCULATING CAVITATION:

H=5.5;    % head of water to center of prop
rho_kgL=1.025;
for i=1:1:length(n)
```

```
sigma07(i)=((188.2+19.62*H)/((Va(i))^2+(4.836*n(i)^2*Dp^2)));
thau07(i)=2*T_S1(i)/(1000*PA*rho_kgL*((Va(i))^2+(4.836*n(i)^2*Dp^2)));
end


Burill=importdata('burill_export_txt.txt');
figure(7)
loglog(Burill(:,1),Burill(:,2),'y')
hold on
loglog(Burill(:,3),Burill(:,4),'m')
loglog(Burill(:,5),Burill(:,6),'c')
loglog(Burill(:,7),Burill(:,8),'r')
loglog(Burill(:,9),Burill(:,10),'Color',[1,0.8,0.6])
loglog(Burill(:,11),Burill(:,12),'g')
loglog(Burill(:,13),Burill(:,14),'b')
loglog(Burill(:,15),Burill(:,16),'k')
loglog(sigma07,thau07,'b.-')
legend('2.5% back cavitation','5% back cavitation','10% back
cavitation','20% back cavitation','30% back cavitation','min
limit','max limit','war-ship','A.E DDG51 ','Location','SouthEast')
grid on
xlabel('sigma')
ylabel('Tau')
axis([0.05 2.0 0.05 0.5])
hold on



for i=1:1:length(n)
    for j=1:1:5
    Q(i,j)=Kq1(i)*rho_sw*n(i)^2*Dp^5;
    P(i,j)=0.97*NS(i)*(2*pi*n(i)*Q(i,j)*1.341/(1000));          %Power
for ship in HP
    P1(i,j)=P(i,j)/2;                                           %Power
per one electric motor
    P1(isnan(P1))=0;
    end

end
P1;

%Electric Motor Efficienct interpolation:

Pmm=[0.85 0.89 0.90 0.91 0.92 0.94 0.94 0.94];
Power=[108 867 2925 3550 6933 13542 23400 30000];
Etha_pmm=pchip(Power,Pmm,P1);
Etha_pmm(isnan(Etha_pmm))=1;

%Total propultion break power calculation

for i=1:1:length(n)
    for j=1:1:5
    TBP(i,j)= P(i,j)/(etha_r*etha_h*Etha_pmm(i));
%break power needed for propulsion per shaft
    TBP(isnan(TBP))=0;
    %TBP(i,j)=BP_S1(i,j)*NS(i);
```

```
%Total propulsion power
    PPE(i,j)=TBP(i,j)/N_GT(i,j);
%Power per gas turbine (total/#of turbines)
    P_CHECK(i,j)=EHP(i)/(etha_00(i)*etha_h*etha_r);
    XXX(i,j)=P_CHECK(i,j)/P(i,j);
    end
end
PPE(isnan(PPE))=0;
TBP(1)=0;



%_____________________________________________________________________
___

%Fuel efficiency for MVDC propulsion (Minimum values for) :


sfc_power=[925.985 1500.341 2071.479 3049.242 4025.615 5899.941 7540
9151.668 13051.87 16055 20760 23841.914 27000.316]; %from SFC curve -
minimum points
SFC=[1.5 1.2 1.0 0.8 0.7 0.6 0.55 0.5 0.45 0.425 0.4 0.39 0.38];
eff_mvdc=1/0.94;
%Data from Julie
%Fitting a curve

%SFC_pchip =   pchip(sfc_power,SFC,PPE);  % Piecewise Cubic Hermite
Interpolating Polynomial -- very safe way to extrapolate data
%SFC_intrp = interp1(sfc_power,SFC,PPE,'linear','extrap');  % linear
interpolation/extrapolation


%Fuel efficiency for MVAC propulsion(Constent turbine rpm=3600):

sfc_power1=[1798.342 2401.73 3169.678 4486.158 5747.782 7880.051
9038.964 11068.52 14579.076 17266.877 21435.695 23958.918 27085.496];
SFC1=[1.5 1.2 1 0.8 0.7 0.6 0.55 0.5 0.45 0.425 0.4 0.39 0.38];
eff_mvac=1/0.98;
%Data from Julie

%SFC_pchip =   pchip(sfc_power1,SFC1,PPE);  % Piecewise Cubic Hermite
Interpolating Polynomial --% very safe way to extrapolate data
%SFC_intrp = interp1(sfc_power1,SFC1,PPE,'linear','extrap');  % linear
interpolation/extrapolation


%SFC_speed1=interp1(sfc_power1,SFC1,PPE) %SFC - lb/hp-hr

figure(6)
plot(sfc_power,SFC)
hold on
plot(sfc_power1,SFC1,'r')
plot(sfc_power,SFC,'b')
xlabel('Power(HP)')
ylabel('S.F.C (lb/HP*hr)')
```

```
legend('MVDC','MVAC')
%scatter(PPE,SFC_pchip,'ro')
%scatter(PPE,SFC_intrp,'bs')


%_____________________________________________________________________
___

%Statistics battle condition/speed/percentage
%battle BC=5
%wartime cruise BC=4
%peacetime cruise BC=3
%anchor BC=2
%shore Bc=1

%The statistic data matrix:

SM=0.01*[53 1.58 0 0 0 ;0 0 6.79 5.15 0.11;0 0 4.74 3.59 0.07;0 0 6.4
4.86 0.1;0 0 6.02 4.57 0.09;0 0 1.54 1.17 0.02;0 0 0.13 0.1 0];

%_____________________________________________________________________
___

%Electrical power only

EP=[0 6000 11000 13000 14000;0 6000 11000 13000 14000;0 6000 11000
13000 14000;0 6000 11000 13000 14000;0 6000 11000 13000 14000;0 6000
11000 13000 14000;0 6000 11000 13000 14000];

%EP_kw=hp2kw*EP_hp;

for j=1:1:5
    for i=1:1:length(Vs)
        TEP_mvdc(i,j)=EP(i,j)*eff_mvdc+TBP(i,j);            %no 20%
margin on electric power
        TEP_p1_mvdc(i,j)=TEP_mvdc(i,j)/N_GT(i,j);           %total
electrical and propulsion power per engine

        TEP_mvac(i,j)=EP(i,j)*eff_mvac+TBP(i,j);            %no 20%
margin on electric power
        TEP_p1_mvac(i,j)=TEP_mvac(i,j)/N_GT(i,j);           %total
electrical and propulsion power per engine

    end
end
TEP_mvdc(:,1)=0;
TEP_mvac(:,1)=0;

TEP_p1_mvdc(:,1)=0;
TEP_p1_mvac(:,1)=0;

for i=2:1:7
    TEP_mvdc(i,2)=0;
    TEP_p1_mvdc(i,2)=0;
```

```
    TEP_mvac(i,2)=0;
    TEP_p1_mvac(i,2)=0;

end


SFC_total_mvdc= pchip(sfc_power,SFC,TEP_p1_mvdc);      %SFC - lb/hp-hr
for MVDC
SFC_total_mvac= pchip(sfc_power1,SFC1,TEP_p1_mvac);    %SFC - lb/hp-hr
for MVAC


for j=1:1:5
    for i=1:1:length(Vs)

Total_fuel_MVDC(i,j)=SFC_total_mvdc(i,j)*SM(i,j)*TEP_p1_mvdc(i,j)*N_GT(
i,j)*0.00045359237;   %total fuel use in mTON per hour operational
profile use

Total_fuel_MVAC(i,j)=SFC_total_mvac(i,j)*SM(i,j)*TEP_p1_mvac(i,j)*N_GT(
i,j)*0.00045359237;   %total fuel use in mTON per hour operational
profile use
    end
end


%Annual use MVDC:
fprintf('The Annual Fuel Consumption For MVDC \n')
Total_fuel_MVDC(isnan(Total_fuel_MVDC))=1;
Total_fuel_MVDC
Annual_use_MVDC=sum(Total_fuel_MVDC(:))*365*24

%Annual use MVAC:
fprintf('The Annual Fuel Consumption For MVAC  \n')
Total_fuel_MVAC(isnan(Total_fuel_MVAC))=1;
Total_fuel_MVAC
Annual_use_MVAC=sum(Total_fuel_MVAC(:))*365*24


%Percenatge of fuel per Speed:

total_fuel_per_state_mvdc=100*Total_fuel_MVDC.*365*24/Annual_use_MVDC
total_fuel_per_state_mvac=100*Total_fuel_MVAC.*365*24/Annual_use_MVAC

total_p_mvdc=sum(total_fuel_per_state_mvdc(:));
%check for sum of 100%
total_p_mvac=sum(total_fuel_per_state_mvac(:));
%check for sum of 100%

X_factor=total_fuel_per_state_mvac./total_fuel_per_state_mvdc;

total_hrs=365*24*sum(SM(:))-365*24*SM(1,1)


%_____________________________________________________________________
```

```
___
%Edurance fuel consumption 20kts for 5000NM

ss_factor=1.1;          %sea state factor

v_ind=5;
C=3;

End_time=5000/20;
Endurance_fuel_MVDC=End_time*SFC_total_mvdc(v_ind,C)*TEP_p1_mvdc(v_ind,
C)*N_GT(v_ind,C)*0.4536/1000; %metric tonns
Endurance_Tankage_MVDC=ss_factor*1.05*Endurance_fuel_MVDC;


Endurance_fuel_MVAC=End_time*SFC_total_mvac(v_ind,C)*TEP_p1_mvac(v_ind,
C)*N_GT(v_ind,C)*0.4536/1000; %metric tonns
Endurance_Tankage_MVAC=ss_factor*1.05*Endurance_fuel_MVAC;

fprintf('The Fuel Consumption For Endurance MVDC(250 hours at 20
kts)is: ')
Endurance_fuel_MVDC

fprintf('\n The tankage for endurance MVDC is: ')
Endurance_Tankage_MVDC

fprintf('\n The Fuel Consumption For Endurance (250 hours at 20 kts)is:
')
Endurance_fuel_MVAC

fprintf('\n The tankage for endurance MVAC is: ')
Endurance_Tankage_MVAC


fprintf('the ratio between the MVAC and MVDC SCFs:')
SFC_ratio=SFC_total_mvac./SFC_total_mvdc

%%Surge to theatre fuel consumption 30kts for 2000NM
%fprintf('Surge to theatre (30kts fo 2000NM) fuel tankage:')
End_time_1=2000/30;
Endurance_fuel_MVDC=End_time_1*SFC_total_mvdc(7,C)*TEP_p1_mvdc(7,C)*N_G
T(7,C)*0.4536/1000; %metric tonns
Surge_to_theatre_Tankage_MVDC=ss_factor*1.05*Endurance_fuel_MVDC;

Endurance_fuel_MVAC=End_time_1*SFC_total_mvac(7,C)*TEP_p1_mvac(7,C)*N_G
T(7,C)*0.4536/1000; %metric tonns
Surge_to_theatre_Tankage_MVAC=ss_factor*1.05*Endurance_fuel_MVAC;
```

Appendix B – Ship Load Distribution Efficiencies

							MVAC				MVDC			
Equipment Name	Anchor (kW)	Cruise (kW)	WarCruise (kW)	Battle (kW)	MVAC eta	MVDC eta	Anchor (kW)	Cruise (kW)	WarCruise (kW)	Battle (kW)	Anchor (kW)	Cruise (kW)	WarCruise (kW)	Battle (kW)
Load_DC_Z1L1_V	35	75	75	75	0.97	0.9409	36.08247423	77.31958763	77.31958763	77.31958763	37.19842704	79.71091508	79.71091508	79.71091508
Load_DC_Z1L2_V	0	300	300	300	0.97	0.9409	0	309.2783505	309.2783505	309.2783505	0	318.8436603	318.8436603	318.8436603
Load_AC_Z1L3_V	320	300	300	300	0.99	0.912673	323.2323232	303.030303	303.030303	303.030303	350.6184581	328.7048045	328.7048045	328.7048045
Load_AC_Z1L4_V	195	200	200	200	0.99	0.912673	196.969697	202.020202	202.020202	202.020202	213.6581229	219.1365363	219.1365363	219.1365363
Load_AC_Z1L5_NV	137.5	435	435	435	0.99	0.912673	138.8888889	439.3939394	439.3939394	439.3939394	150.6563687	476.6219665	476.6219665	476.6219665
Load_AC_Z1L6_NV	3.5	0	0	0	0.99	0.912673	3.535353535	0	0	0	3.834889385	0	0	0
Load_DC_Z2L1_NV	0	0	0	0	0.97	0.9409	0	0	0	0	0	0	0	0
Load_DC_Z2L2_V	10	40	40	40	0.97	0.9409	10.30927835	41.2371134	41.2371134	41.2371134	10.62812201	42.51248804	42.51248804	42.51248804
Load_AC_Z2L3_V	465	700	700	700	0.99	0.912673	469.6969697	707.0707071	707.0707071	707.0707071	509.4924469	766.9778771	766.9778771	766.9778771
Load_AC_Z2L4_V	150	375	375	375	0.99	0.912673	151.5151515	378.7878788	378.7878788	378.7878788	164.3524022	410.8810056	410.8810056	410.8810056
Load_AC_Z2L5_NV	200	180	180	180	0.99	0.912673	202.020202	181.8181818	181.8181818	181.8181818	219.1365363	197.2228827	197.2228827	197.2228827
Load_AC_Z2L6_NV	17.5	20	20	20	0.99	0.912673	17.67676768	20.2020202	20.2020202	20.2020202	19.17444693	21.91365363	21.91365363	21.91365363
Load_DC_Z3L1_V	10	20	20	20	0.97	0.9409	10.30927835	20.6185567	20.6185567	20.6185567	10.62812201	21.25624402	21.25624402	21.25624402
Load_AC_Z3L2_V	600	600	600	600	0.99	0.9312	606.0606061	606.0606061	606.0606061	606.0606061	644.3298969	644.3298969	644.3298969	644.3298969
Load_AC_Z3L3_V	275	950	950	950	0.99	0.912673	277.7777778	959.5959596	959.5959596	959.5959596	301.3127374	1040.898547	1040.898547	1040.898547
Load_AC_Z3L4_NV	187.5	375	375	375	0.99	0.912673	189.3939394	378.7878788	378.7878788	378.7878788	205.4405028	410.8810056	410.8810056	410.8810056
Load_AC_Z3L5_NV	2	0	0	0	0.99	0.912673	2.02020202	0	0	0	2.191365363	0	0	0
Load_DC_Z4L1_V	0	30	30	30	0.97	0.9409	0	30.92783505	30.92783505	30.92783505	0	31.88436603	31.88436603	31.88436603
Load_AC_Z4L2_V	100	240	240	240	0.99	0.912673	101.010101	242.4242424	242.4242424	242.4242424	109.5682682	262.9638436	262.9638436	262.9638436
Load_AC_Z4L3_V	207.5	825	825	825	0.99	0.912673	209.5959596	833.3333333	833.3333333	833.3333333	227.3541564	903.9382123	903.9382123	903.9382123
Load_AC_Z4L4_NV	110	335	335	335	0.99	0.912673	111.1111111	338.3838384	338.3838384	338.3838384	120.525095	367.0536983	367.0536983	367.0536983
Load_AC_Z4L5_NV	2	0	0	0	0.99	0.912673	2.02020202	0	0	0	2.191365363	0	0	0
Load_DC_Z5L1_V_Radar	2000	3000	3000	3000	0.97	0.97	2061.85567	3092.783505	3092.783505	3092.783505	2061.85567	3092.783505	3092.783505	3092.783505
Load_DC_V_Pulse	0	2000	4000	5000	0.97	0.97	0	2061.85567	4123.71134	5154.639175	0	2061.85567	4123.71134	5154.639175
	5,028	11,000	13,000	14,000			5,121	11,225	13,287	14,318	5,364	11,700	13,762	14,793
	6000	11000	13000	14000			0.982	0.980	0.978	0.978	0.937	0.940	0.945	0.946
										0.98				**0.94**